Journal of Computational Mathematics
Vol.xx, No.x, 2023, 1–20.

http://www.global-sci.org/jcm
doi:10.4208/jcm.2304-m2022-0185

THE NYSTRÖM METHOD FOR ELASTIC WAVE SCATTERING BY UNBOUNDED ROUGH SURFACES*

Jianliang Li
Key Laboratory of Computing and Stochastic Mathematics, School of Mathematics and Statistics, Hunan Normal University, Changsha, Hunan 410081, China
Email: lijl@amss.ac.cn
Xiaoli Liu[1)]
School of Mathematical Sciences, Beihang University, Beijing 100191, China
Email: xiaoli_liu@buaa.edu.cn
Bo Zhang
LSEC and Academy of Mathematics and Systems Science, Chinese Academy of Sciences, Beijing 100190, China
School of Mathematical Sciences, University of Chinese Academy of Sciences, Beijing 100049, China
Email: b.zhang@amt.ac.cn
Haiwen Zhang
Academy of Mathematics and Systems Science, Chinese Academy of Sciences, Beijing 100190, China
Email: zhanghaiwen@amss.ac.cn

Abstract

We consider a numerical algorithm for the two-dimensional time-harmonic elastic wave scattering by unbounded rough surfaces with Dirichlet boundary condition. A Nyström method is proposed for the scattering problem based on the integral equation method. Convergence of the Nyström method is established with convergence rate depending on the smoothness of the rough surfaces. In doing so, a crucial role is played by analyzing the singularities of the kernels of the relevant boundary integral operators. Numerical experiments are presented to demonstrate the effectiveness of the method.

Mathematics subject classification: 35P25, 45P05.
Key words: Elastic wave scattering, Unbounded rough surface, Nyström method.

1. Introduction

We consider the two-dimensional time-harmonic elastic scattering problem for unbounded rough surfaces with Dirichlet boundary condition. This kind of problem has attracted much attention since it has a wide range of applications in diverse scientific areas such as seismology and non-destructive testing.

Given the incident wave and the rough surface, the direct scattering problem is to determine the distribution of the scattered wave and develop an efficient algorithm to simulate the scattered wave. The well-posedness of the acoustic scattering problems by unbounded rough surfaces have been extensively studied via either a variational approach [5,8–10] or the integral equation method [11,12,26,27,29] based on the classical Fredholm theory [15,22] or the generalized Fredholm theory [13]. When applying the integral equation method, the direct scattering

* Received August 7, 2022 / Revised version received October 31, 2022 / Accepted April 19, 2023 / Published online November 15, 2023 /
1) Corresponding author

problem can be transformed to an equivalent second-kind integral equation with logarithmic singular periodic kernels. One of the most efficient method for the numerical solution to this kind of integral equation is the Nyström method, which was first applied to the acoustic scattering by sound-soft obstacles [14], and has been extended to acoustic scattering by sound-hard obstacles [19]. Compared with the second-kind integral equation defined on a finite interval, a non-trivial extension of the Nyström method is the work [25], which has extended it to deal with the second-kind integral equation defined on the real line. Thus, it enables us to obtain the numerical solution of the acoustic scattering problems by unbounded rough surfaces, see [20,25] for the sound-soft case and [21] for the penetrable case.

Although a large number of results have been obtained for the acoustic case, there are few available results for elastic scattering by unbounded rough surfaces, especially for the computational aspect. The unique solvability of the elastic scattering by rough surfaces with Dirichlet boundary conditions has been established in [2], while the existence result was given in [3] using the boundary integral equation method (see also [1] for a comprehensive discussion). The authors in [18] studied the well-posedness of the elastic scattering problem by unbounded rough surfaces via the variational approach. Some numerical algorithms are proposed to solve elastic scattering problems while the scatterers are bounded obstacles, such as boundary element method [6,7], spectral algorithm [17,23] and Nyström method [16,28]. However, to the best of our knowledge, few numerical algorithms are presented for elastic wave scattering by unbounded rough surfaces.

The purpose of this paper is to develop the Nyström method for two-dimensional time-harmonic elastic scattering problem for unbounded rough surfaces with Dirichlet boundary condition. Our method is based on the integral equation formulations given in [1, 3], which can be reduced to a class of integral equations on the real line. A crucial role of our method is played by a thorough analysis on the singularities of the kernels in the relevant integral equations, which involves the Green tensor for Navier equation in the half-space. By splitting off the logarithmic singularity in the related kernels and using the asymptotic behaviour of the Bessel functions, we obtain the convergence of the Nyström method with convergence rate depending on the smoothness of the rough surfaces. Several numerical examples are presented to verify our theoretical results and show the effectiveness of our method.

The paper is organized as follows. In Section 2, we give a brief introduction to a mathematical model of the scattering problem and present the existed well-posedness result using the integral equation method. Section 3 is devoted to analyzing the singularities for the relevant kernels included in the integral expression of the solution. In Section 4, we establish the convergence of the Nyström method. Numerical experiments are given to show the effectiveness of the proposed method in Section 5. Finally, we give a conclusion in Section 6.

2. The Well-Posedness of the Scattering Problem

In this section, we present the existed results for the well-posedness of the two-dimensional elastic wave scattering problem by unbounded rough surfaces. First, we introduce some notations and function spaces used throughout this paper. We will use bold lowercase letters to denote all vectors and vector fields, and use bold capital letters to denote matrices or matrix functions. For a vector $\mathbf{a} = (\mathrm{a}_1, \mathrm{a}_2)^\top$, we define $\mathbf{a}^\perp = (\mathrm{a}_2, -\mathrm{a}_1)^\top$ which is orthogonal to $\mathbf{a}$, and unless otherwise stated, we use $|\mathbf{a}|$ to denote its Euclidean norm. For any $b \in \mathbb{R}$, we define the

half-space U_b and its boundary Γ_b as

$$U_b := \left\{\mathbf{x} \in \mathbb{R}^2 : \mathrm{x}_2 > b\right\}, \quad \Gamma_b := \left\{\mathbf{x} \in \mathbb{R}^2 : \mathrm{x}_2 = b\right\}.$$

The notations J_n and Y_n are Bessel functions and Neumann functions of order n, respectively. The linear combination

$$H_n^{(1)} := J_n + \mathrm{i}Y_n$$

is known as the Hankel function of the first kind of order n. Finally, we introduce some function spaces. For $V \subset \mathbb{R}^m, m = 1, 2$, let $BC(V)$ represent the set of bounded and continuous complex-valued functions on V under the norm $\|\varphi\|_{\infty,V} := \sup_{\mathbf{x}\in V} |\varphi(\mathbf{x})|$. We denote by $BC^n(\mathbb{R}^m)$ the set of all functions whose derivatives up to order n are bounded and continuous on $\mathbb{R}^m$ with the norm

$$\|\varphi\|_{BC^n(\mathbb{R}^m)} := \max_{j=0,1,\ldots,n} \max_{|\boldsymbol{\alpha}|=j} \left\|\partial_{\mathbf{x}}^{\boldsymbol{\alpha}}\varphi\right\|_{\infty,\mathbb{R}^m},$$

where $\boldsymbol{\alpha} = (\alpha_1, \alpha_2, \cdots, \alpha_m)$ and $|\boldsymbol{\alpha}| := \sum_{i=1}^m \alpha_i$. Let $H^1(V)$ and $H^{1/2}(\partial V)$ be the standard Sobolev spaces for any open set $V \subset \mathbb{R}^m$ provided the boundary of V is smooth enough. The notations $H^1_{\mathrm{loc}}(V)$ and $H^{1/2}_{\mathrm{loc}}(V)$ stand for the set of functions which are elements of $H^1(\mathcal{V})$ and $H^{1/2}(\mathcal{V})$ for any $\mathcal{V} \subset\subset V$, respectively. Here the notation $\mathcal{V} \subset\subset V$ denotes that the closure of $\mathcal{V}$ is a compact subset of V.

For theoretical analysis in Sections 2-4, without loss of generality, we assume that the rough surface Γ lies above the x_1-axis and can be described as

$$\Gamma := \left\{(\mathrm{x}_1, \mathrm{x}_2) \in \mathbb{R}^2 : \mathrm{x}_2 = f(\mathrm{x}_1)\right\},$$

where $f \in B^{(n)}_{c_1,c_2}$ with

$$B^{(n)}_{c_1,c_2} := \left\{f \in BC^n(\mathbb{R}) : \|f\|_{BC^n(\mathbb{R})} \le c_1 \ \text{ and } \ \inf_{\mathrm{x}_1\in\mathbb{R}} f(\mathrm{x}_1) \ge c_2\right\}$$

for some non-negative integer n, some constants $c_1 > 0$ and $c_2 > 0$. The whole space is separated by Γ into two unbounded half-spaces and the upper one is denoted by

$$\Omega := \left\{(\mathrm{x}_1, \mathrm{x}_2) \in \mathbb{R}^2 : \mathrm{x}_2 > f(\mathrm{x}_1)\right\}.$$

Throughout the paper, we set $h \in \mathbb{R}$ such that $h < \inf_{\mathrm{x}_1\in\mathbb{R}} f(\mathrm{x}_1)$. For $\mathbf{y} = (\mathrm{y}_1, \mathrm{y}_2) \in U_h$, its image under a reflection with respect to Γ_h is defined by $\mathbf{y}' := (\mathrm{y}_1, 2h - \mathrm{y}_2)$. See Fig. 2.1 for the problem geometry.

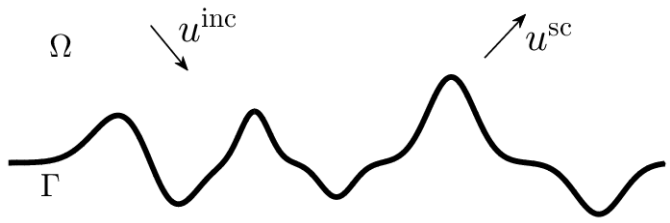

Fig. 2.1. Physical configuration of the scattering problem by a rough surface.

Suppose an incoming field $\boldsymbol{u}^{\rm inc} = (u_1^{\rm inc}, u_2^{\rm inc})$ is incident on the infinite surface Γ from the upper region Ω. Then the scattering of $\boldsymbol{u}^{\rm inc}$ by the infinite rough surface Γ can be modelled by the two-dimensional Navier equation

$$\mu\Delta\boldsymbol{u}^{\rm sc} + (\lambda+\mu)\nabla\nabla\cdot\boldsymbol{u}^{\rm sc} + \omega^2\boldsymbol{u}^{\rm sc} = 0 \quad \text{in } \Omega, \tag{2.1}$$

where $\boldsymbol{u}^{\rm sc} = (u_1^{\rm sc}, u_2^{\rm sc})$ is the scattered field, $\omega > 0$ represents the angular frequency, and λ and μ are the Lamé constants satisfying $\mu > 0$ and $\lambda + 2\mu > 0$, which leads to that the second-order partial differential operator $\Delta^* := \mu\Delta + (\lambda+\mu)\nabla\nabla$ is strongly elliptic [24]. Let $\boldsymbol{u} := \boldsymbol{u}^{\rm inc} + \boldsymbol{u}^{\rm sc}$ denote the total field consisting of the incident field and the scattered field. Further, the Dirichlet boundary condition is imposed on Γ, that is

$$\boldsymbol{u}^{\rm sc} = -\boldsymbol{u}^{\rm inc} \quad \text{on } \Gamma. \tag{2.2}$$

Since the Navier equation (2.1) is imposed in the unbounded region Ω, an appropriate radiation condition is needed for the considered scattering problem. To this end, we first introduce the generalized stress vector $\boldsymbol{P}$ which is defined on a curve $\Lambda \in \mathbb{R}^2$ with $\boldsymbol{\nu}$ being the unit normal on Λ. For a vector $\boldsymbol{\varphi}$, $\boldsymbol{P\varphi}$ is also a vector defined by

$$\boldsymbol{P\varphi} := (\mu+\widetilde{\mu})\frac{\partial\boldsymbol{\varphi}}{\partial\nu} + \widetilde{\lambda}\boldsymbol{\nu}\mathrm{div}\boldsymbol{\varphi} - \widetilde{\mu}\boldsymbol{\nu}^{\perp}\mathrm{div}^{\perp}\boldsymbol{\varphi} \tag{2.3}$$

with $\widetilde{\lambda}$, $\widetilde{\mu} \in \mathbb{R}$ satisfying $\widetilde{\lambda} + \widetilde{\mu} = \lambda + \mu$ and

$$\mathrm{div}^{\perp}\boldsymbol{\varphi} := \frac{\partial\varphi_1}{\partial \mathrm{x}_2} - \frac{\partial\varphi_2}{\partial \mathrm{x}_1}, \quad \boldsymbol{\varphi} = (\varphi_1, \varphi_2)^{\top}.$$

For a matrix $\boldsymbol{M}$, $\boldsymbol{PM}$ is also a matrix whose element is defined by

$$(\boldsymbol{PM})_{jk} = \big(\boldsymbol{P}(\boldsymbol{M}_{\boldsymbol{j}.})^{\top}\big)_k, \quad j,k = 1,2.$$

In this paper, the scattered wave is assumed to satisfy the following upwards propagating radiation condition (UPRC) [3]:

$$\boldsymbol{u}^{\rm sc}(\mathbf{x}) = \int_{\Gamma_H} \boldsymbol{\Pi}_H(\mathbf{x},\mathbf{y})\boldsymbol{\phi}(\mathbf{y})ds(\mathbf{y}), \quad \mathbf{x} \in U_H \tag{2.4}$$

for some $\boldsymbol{\phi} \in [L^{\infty}(\Gamma_H)]^2$ with $H > \sup_{\mathrm{x}_1\in\mathbb{R}} f(\mathrm{x}_1)$, where the kernel $\boldsymbol{\Pi}_H(\mathbf{x},\mathbf{y})$ in (2.4) is a matrix function given by

$$\boldsymbol{\Pi}_H(\mathbf{x},\mathbf{y}) = \boldsymbol{P}^{(\mathbf{y})}\boldsymbol{G}_H(\mathbf{x},\mathbf{y}) \tag{2.5}$$

with $\boldsymbol{\nu}$ in (2.5) being the upward unit normal on Γ_H and $\boldsymbol{G}_H$ being the Green's tensor of the Navier equation (2.1) in U_H with Dirichlet boundary condition on Γ_H, which is given by

$$\boldsymbol{G}_H(\mathbf{x},\mathbf{y}) := \boldsymbol{\Psi}(\mathbf{x},\mathbf{y}) - \boldsymbol{\Psi}(\mathbf{x},\mathbf{y}') + \boldsymbol{U}(\mathbf{x},\mathbf{y}), \quad \mathbf{x},\mathbf{y} \in U_H, \quad \mathbf{x} \neq \mathbf{y}. \tag{2.6}$$

Here, $\boldsymbol{\Psi}$ is the Green's tensor for the Navier equation (2.1) in free space $\mathbb{R}^2$, which is defined by

$$\boldsymbol{\Psi}(\mathbf{x},\mathbf{y}) = \frac{1}{\mu}\Phi(\mathbf{x},\mathbf{y},\kappa_{\rm s})\boldsymbol{I} + \frac{1}{\omega^2}\nabla_{\mathbf{x}}\nabla_{\mathbf{x}}^{\top}\big(\Phi(\mathbf{x},\mathbf{y},\kappa_{\rm s}) - \Phi(\mathbf{x},\mathbf{y},\kappa_{\rm p})\big), \quad \mathbf{x},\mathbf{y} \in \mathbb{R}^2, \quad \mathbf{x} \neq \mathbf{y} \tag{2.7}$$

with $\kappa_{\rm s}$ and $\kappa_{\rm p}$ being the shear and compressional wavenumbers defined by

$$\kappa_{\rm s} := c_{\rm s}\omega, \quad \kappa_{\rm p} := c_{\rm p}\omega, \quad c_{\rm s} := \mu^{-\frac{1}{2}}, \quad c_{\rm p} := (\lambda+2\mu)^{-\frac{1}{2}},$$

and

$$\Phi(\mathbf{x},\mathbf{y},\kappa) := \frac{\mathrm{i}}{4}H_0^{(1)}(\kappa|\mathbf{x}-\mathbf{y}|)$$

being the fundamental solution for the two-dimensional Helmholtz equation with $H_0^{(1)}$ to be the Hankel function of the first kind of order 0. And $\boldsymbol{U}(\mathbf{x},\mathbf{y})$ in (2.6) is a matrix function defined by

$$\boldsymbol{U}(\mathbf{x},\mathbf{y}) = -\frac{\mathrm{i}}{2\pi\omega^2}\int_{\mathbb{R}}[\boldsymbol{M}_{\mathrm{p}}(\tau,\gamma_{\mathrm{p}},\gamma_{\mathrm{s}};\mathrm{x}_2,\mathrm{y}_2)+\boldsymbol{M}_{\mathrm{s}}(\tau,\gamma_{\mathrm{p}},\gamma_{\mathrm{s}};\mathrm{x}_2,\mathrm{y}_2)]e^{-\mathrm{i}(\mathrm{x}_1-\mathrm{y}_1)\tau}d\tau,$$

where

$$\gamma_{\mathrm{p}} := \sqrt{\kappa_{\mathrm{p}}^2-\tau^2}, \quad \gamma_{\mathrm{s}} := \sqrt{\kappa_{\mathrm{s}}^2-\tau^2},$$

and

$$\boldsymbol{M}_{\mathrm{p}}(\tau,\gamma_{\mathrm{p}},\gamma_{\mathrm{s}};\mathrm{x}_2,\mathrm{y}_2) := \frac{e^{\mathrm{i}\gamma_{\mathrm{p}}(\mathrm{x}_2+\mathrm{y}_2-2H)}-e^{\mathrm{i}(\gamma_{\mathrm{p}}(\mathrm{x}_2-H)+\gamma_{\mathrm{s}}(\mathrm{y}_2-H))}}{\gamma_{\mathrm{p}}\gamma_{\mathrm{s}}+\tau^2}\begin{bmatrix}-\tau^2\gamma_{\mathrm{s}} & \tau^3\\ \tau\gamma_{\mathrm{p}}\gamma_{\mathrm{s}} & -\tau^2\gamma_{\mathrm{p}}\end{bmatrix},$$

$$\boldsymbol{M}_{\mathrm{s}}(\tau,\gamma_{\mathrm{p}},\gamma_{\mathrm{s}};\mathrm{x}_2,\mathrm{y}_2) := \frac{e^{\mathrm{i}\gamma_{\mathrm{s}}(\mathrm{x}_2+\mathrm{y}_2-2H)}-e^{\mathrm{i}(\gamma_{\mathrm{s}}(\mathrm{x}_2-H)+\gamma_{\mathrm{p}}(\mathrm{y}_2-H))}}{\gamma_{\mathrm{p}}\gamma_{\mathrm{s}}+\tau^2}\begin{bmatrix}-\tau^2\gamma_{\mathrm{s}} & -\tau\gamma_{\mathrm{p}}\gamma_{\mathrm{s}}\\ -\tau^3 & -\tau^2\gamma_{\mathrm{p}}\end{bmatrix}.$$

With the aid of [3, Theorem 2.1], we have $\boldsymbol{U}(\mathbf{x},\mathbf{y})\in[C^\infty(U_H)\cap C^1(\overline{U_H})]^{2\times 2}$, which will be used in the analysis on the convergence of the Nyström method. We refer to [1,2] for more properties of the UPRC, and its relation to the Rayleigh expansion radiation condition for diffraction grating and the Kupradze's radiation condition for the scattering by bounded obstacles.

To ensure the uniqueness of the scattering problem, we also need the following vertical growth rate condition:

$$\sup_{\mathbf{x}\in\Omega}|\mathrm{x}_2|^{\beta}|\boldsymbol{u}^{\mathrm{sc}}(\mathbf{x})|<\infty \quad \text{for some} \quad \beta\in\mathbb{R}. \tag{2.8}$$

In summary, the scattering problem (2.1)-(2.4) and (2.8) can be described by the following boundary value problem with $\boldsymbol{g} = -\boldsymbol{u}^{\mathrm{inc}}|_\Gamma$.

Dirichlet Problem (DP): Given $\boldsymbol{g}\in[BC(\Gamma)\cap H^{1/2}_{\mathrm{loc}}(\Gamma)]^2$, find $\boldsymbol{u}^{\mathrm{sc}}\in\left[C^2(\Omega)\cap C(\overline{\Omega})\cap H^1_{\mathrm{loc}}(\Omega)\right]^2$ such that

1. $\boldsymbol{u}^{\mathrm{sc}}$ is a solution of the Navier equation (2.1) in Ω.
2. $\boldsymbol{u}^{\mathrm{sc}}$ satisfies the Dirichlet boundary condition $\boldsymbol{u}^{\mathrm{sc}}=\boldsymbol{g}$ on Γ.
3. $\boldsymbol{u}^{\mathrm{sc}}$ satisfies the UPRC (2.4).
4. $\boldsymbol{u}^{\mathrm{sc}}$ satisfies the vertical growth rate condition (2.8).

The following uniqueness result has been proved in [2, Theorem 4.6] for the problem (DP).

Theorem 2.1 ([2, Theorem 4.6]). *The problem (DP) has at most one solution.*

The existence of the solution to the problem (DP) has been investigated in [3] by integral equation method. The main idea is to seek for a solution in the form of a combined single- and double-layer potential

$$\boldsymbol{u}^{\mathrm{sc}}(\mathbf{x}) = \int_\Gamma\left[\boldsymbol{\Pi}_h(\mathbf{x},\mathbf{y})-\mathrm{i}\eta\boldsymbol{G}_h(\mathbf{x},\mathbf{y})\right]\boldsymbol{\psi}(\mathbf{y})ds(\mathbf{y}), \quad \mathbf{x}\in\Omega, \tag{2.9}$$

where $\mathbf{\Pi}_h(\mathbf{x},\mathbf{y})$ is defined similar as $\mathbf{\Pi}_H(\mathbf{x},\mathbf{y})$ in (2.4) with $h < \inf \mathrm{x}_1 \in \mathbb{R} f(\mathrm{x}_1)$ and $\boldsymbol{\nu}$ being the unit normal on Γ pointing to Ω, $\boldsymbol{G}_h(\mathbf{x},\mathbf{y})$ is defined similar as $\boldsymbol{G}_H(\mathbf{x},\mathbf{y})$ in (2.6), and for simplicity, we will write $\mathbf{\Pi}(\mathbf{x},\mathbf{y})$ and $\boldsymbol{G}(\mathbf{x},\mathbf{y})$ for $\mathbf{\Pi}_h(\mathbf{x},\mathbf{y})$ and $\boldsymbol{G}_h(\mathbf{x},\mathbf{y})$, respectively, if there is no misleading, $\boldsymbol{\psi} \in [BC(\Gamma) \cap H^{1/2}_{\mathrm{loc}}(\Gamma)]^2$ and η is a complex number satisfying $\mathrm{Re}(\eta) > 0$. Throughout this paper, to ensure that $\mathbf{\Pi}(\mathbf{x},\mathbf{y})$ has a weak singularity while $|\mathbf{x}-\mathbf{y}| \to 0$ for $\mathbf{x},\mathbf{y} \in \Gamma$, $\widetilde{\mu}$ and $\widetilde{\lambda}$ in (2.3) are chosen to be

$$\widetilde{\mu} = \frac{\mu(\lambda+\mu)}{\lambda+3\mu}, \quad \widetilde{\lambda} = \frac{(\lambda+\mu)(\lambda+2\mu)}{\lambda+3\mu}. \tag{2.10}$$

Thus, it follows from [3, Theorems 2.6, 2.7, Lemma 2.8] that $\boldsymbol{u}^{\mathrm{sc}}$ given by (2.9) satisfies $\boldsymbol{u}^{\mathrm{sc}} \in [C^2(\Omega) \cap C(\overline{\Omega}) \cap H^1_{\mathrm{loc}}(\Omega)]^2$. By [3, Theorems 2.4, 3.2], it can be deduced that $\boldsymbol{u}^{\mathrm{sc}}$ given by (2.9) satisfies the Navier equation (2.1) and the UPRC (2.4). Further, as a consequence of [3, Theorems 2.1, 2.3], $\boldsymbol{u}^{\mathrm{sc}}$ given by (2.9) satisfies the vertical growth rate condition (2.8) with $\beta = -1/2$.

According to the jump relations for elastic single- and double-layer potentials shown in [3, Theorems 2.6, 2.7], it is easy to see that $\boldsymbol{u}^{\mathrm{sc}}$ given by (2.9) is a solution to the problem (DP) provided $\boldsymbol{\psi}$ is a solution to the following integral equation:

$$\frac{1}{2}\boldsymbol{\psi}(\mathbf{x}) + \int_\Gamma \big[\mathbf{\Pi}(\mathbf{x},\mathbf{y}) - \mathrm{i}\eta \boldsymbol{G}(\mathbf{x},\mathbf{y})\big]\boldsymbol{\psi}(\mathbf{y}) ds(\mathbf{y}) = \boldsymbol{g}(\mathbf{x}), \quad \mathbf{x} \in \Gamma, \tag{2.11}$$

which can be rewritten in the operator form

$$(\boldsymbol{I} + \boldsymbol{D}_\Gamma - \mathrm{i}\eta \boldsymbol{S}_\Gamma)\boldsymbol{\psi} = 2\boldsymbol{g} \quad \text{on } \Gamma, \tag{2.12}$$

where $\boldsymbol{D}_\Gamma$ and $\boldsymbol{S}_\Gamma$ are the elastic double-layer and single-layer operators given by

$$(\boldsymbol{D}_\Gamma \boldsymbol{\psi})(\mathbf{x}) := 2\int_\Gamma \mathbf{\Pi}(\mathbf{x},\mathbf{y})\boldsymbol{\psi}(\mathbf{y}) ds(\mathbf{y}), \quad \mathbf{x} \in \Gamma,$$
$$(\boldsymbol{S}_\Gamma \boldsymbol{\psi})(\mathbf{x}) := 2\int_\Gamma \boldsymbol{G}(\mathbf{x},\mathbf{y})\boldsymbol{\psi}(\mathbf{y}) ds(\mathbf{y}), \quad \mathbf{x} \in \Gamma.$$

For $\mathbf{x},\mathbf{y} \in \Gamma$, we denote

$$\mathbf{x} = \mathbf{x}(s) = \big(s, f(s)\big), \quad \mathbf{y} = \mathbf{y}(t) = \big(t, f(t)\big), \quad \widetilde{\boldsymbol{\psi}}(t) := \boldsymbol{\psi}\big(\mathbf{y}(t)\big), \quad \widetilde{\boldsymbol{g}}(s) := \boldsymbol{g}\big(\mathbf{x}(s)\big).$$

By changing the variables, we rewrite $\boldsymbol{D}_\Gamma$ and $\boldsymbol{S}_\Gamma$ as the following operators:

$$(\boldsymbol{D}\widetilde{\boldsymbol{\psi}})(s) := 2\int_{\mathbb{R}} \mathbf{\Pi}\big(\mathbf{x}(s),\mathbf{y}(t)\big)\widetilde{\boldsymbol{\psi}}(t)\sqrt{1+f'(t)^2}dt, \quad s \in \mathbb{R}, \tag{2.13}$$

$$(\boldsymbol{S}\widetilde{\boldsymbol{\psi}})(s) := 2\int_{\mathbb{R}} \boldsymbol{G}\big(\mathbf{x}(s),\mathbf{y}(t)\big)\widetilde{\boldsymbol{\psi}}(t)\sqrt{1+f'(t)^2}dt, \quad s \in \mathbb{R}. \tag{2.14}$$

Then the solvability of (2.12) in $[BC(\Gamma)]^2$ is equivalent to finding the solution $\widetilde{\boldsymbol{\psi}}$ to the integral equation

$$(\boldsymbol{I} + \boldsymbol{D} - \mathrm{i}\eta \boldsymbol{S})\,\widetilde{\boldsymbol{\psi}} = 2\widetilde{\boldsymbol{g}} \tag{2.15}$$

in $[BC(\mathbb{R})]^2$, which is given in the following theorem.

Theorem 2.2 ([3, Corollary 5.12, Theorem 5.13]). *For any $f \in B^{(2)}_{c_1,c_2}$, the integral operator $\boldsymbol{I} + \boldsymbol{D} - \mathrm{i}\eta\boldsymbol{S} : [BC(\mathbb{R})]^2 \to [BC(\mathbb{R})]^2$ is bijective (and so boundedly invertible) with*

$$\sup_{f \in B^{(2)}_{c_1,c_2}} \big\|(\boldsymbol{I} + \boldsymbol{D} - \mathrm{i}\eta\boldsymbol{S})^{-1}\big\|_{[BC(\mathbb{R})]^2 \to [BC(\mathbb{R})]^2} < \infty.$$

Thus, the integral equations (2.11) *and* (2.15) *have exactly one solution for every* $f \in B^{(2)}_{c_1,c_2}$. *Moreover, we have*

$$|\boldsymbol{u}^{\rm sc}(\mathbf{x})| \le C(\mathrm{x}_2 - h)^{\frac{1}{2}} \|\boldsymbol{g}\|_{\infty,\Gamma}, \quad \mathbf{x} \in \Omega$$

for some constants $C > 0$ *depending only on* $B^{(2)}_{c_1,c_2}$ *and* ω.

Remark 2.1. By Theorems 2.1 and 2.2, the problem (DP) has a unique solution.

3. The Singularity for the Kernel of $\boldsymbol{D} - \mathrm{i}\eta\boldsymbol{S}$

This section is devoted to analyzing the singularity of the boundary integral equation (2.15), which will be used for the further investigation on the Nyström method in Section 4. The main idea is to write the kernel $\boldsymbol{A}(s,t)$ of the integral operator $\boldsymbol{D} - \mathrm{i}\eta\boldsymbol{S}$ in (2.15) in the following form:

$$\boldsymbol{A}(s,t) = \frac{1}{2\pi}\boldsymbol{B}(s,t)\ln\left(4\sin^2\frac{s-t}{2}\right) + \boldsymbol{C}(s,t), \quad s,t \in \mathbb{R}, \quad s \ne t \tag{3.1}$$

with smooth matrix functions $\boldsymbol{B}(s,t) \in [C^n_{0,\pi}(\mathbb{R}^2)]^{2\times 2}$ and $\boldsymbol{C}(s,t) \in [BC^n_p(\mathbb{R}^2)]^{2\times 2}$, where $C^n_{0,\pi}(\mathbb{R}^2)$ and $BC^n_p(\mathbb{R}^2)$ are defined as

$$\begin{aligned} C^n_{0,\pi}(\mathbb{R}^2) &:= \big\{a(s,t) \in BC^n(\mathbb{R}^2) : a(s,t) = 0 \ \text{ for } \ |s-t| \ge \pi\big\},\\ BC^n_p(\mathbb{R}^2) &:= \big\{a(s,t) \in BC^n(\mathbb{R}^2) : \|a\|_{BC^n_p(\mathbb{R}^2)} < \infty\big\} \end{aligned}$$

with the norm

$$\|a\|_{BC^n_p(\mathbb{R}^2)} := \sup_{\substack{j,k=0,\dots,n,\\ j+k\le n}} \left\| \widetilde{w}_p(s,t)\frac{\partial^{j+k}a(s,t)}{\partial^j s\partial^k t}\right\|_\infty,$$

and the weight $\widetilde{w}_p(s,t) := (1+|s-t|)^p$ for some $p > 1$, which are closed subspaces of $BC^n(\mathbb{R}^2)$.

According to (2.5), (2.6), (2.13) and (2.14), the operators $\boldsymbol{D}$ and $\boldsymbol{S}$ can be decomposed into two parts as follows:

$$\boldsymbol{D} = \boldsymbol{D}_1 - \boldsymbol{D}_2, \quad \boldsymbol{S} = \boldsymbol{S}_1 - \boldsymbol{S}_2,$$

where

$$(\boldsymbol{D}_1\widetilde{\boldsymbol{\psi}})(s) := 2\int_{\mathbb{R}} \boldsymbol{\Pi}_1\big(\mathbf{x}(s),\mathbf{y}(t)\big)\widetilde{\boldsymbol{\psi}}(t)\sqrt{1+f'(t)^2}dt, \qquad s \in \mathbb{R}, \tag{3.2}$$

$$(\boldsymbol{D}_2\widetilde{\boldsymbol{\psi}})(s) := 2\int_{\mathbb{R}} \boldsymbol{\Pi}_2\big(\mathbf{x}(s),\mathbf{y}(t)\big)\widetilde{\boldsymbol{\psi}}(t)\sqrt{1+f'(t)^2}dt, \qquad s \in \mathbb{R}, \tag{3.3}$$

$$(\boldsymbol{S}_1\widetilde{\boldsymbol{\psi}})(s) := 2\int_{\mathbb{R}} \boldsymbol{\Psi}\big(\mathbf{x}(s),\mathbf{y}(t)\big)\widetilde{\boldsymbol{\psi}}(t)\sqrt{1+f'(t)^2}dt, \qquad s \in \mathbb{R}, \tag{3.4}$$

$$(\boldsymbol{S}_2\widetilde{\boldsymbol{\psi}})(s) := 2\int_{\mathbb{R}} \big[\boldsymbol{\Psi}\big(\mathbf{x}(s),\mathbf{y}'(t)\big) - \boldsymbol{U}\big(\mathbf{x}(s),\mathbf{y}(t)\big)\big]\widetilde{\boldsymbol{\psi}}(t)\sqrt{1+f'(t)^2}dt, \quad s \in \mathbb{R} \tag{3.5}$$

with the components of $\boldsymbol{\Pi}_1(\mathbf{x},\mathbf{y})$ and $\boldsymbol{\Pi}_2(\mathbf{x},\mathbf{y})$ given by

$$\boldsymbol{\Pi}_1(\mathbf{x},\mathbf{y}) := \boldsymbol{P}^{(\mathbf{y})}\boldsymbol{\Psi}(\mathbf{x},\mathbf{y}), \quad \boldsymbol{\Pi}_2(\mathbf{x},\mathbf{y}) := \boldsymbol{P}^{(\mathbf{y})}\big(\boldsymbol{\Psi}(\mathbf{x},\mathbf{y}') - \boldsymbol{U}(\mathbf{x},\mathbf{y})\big). \tag{3.6}$$

Hence, the integral equation (2.15) can be rewritten as

$$[\boldsymbol{I} + \boldsymbol{D}_1 - \mathrm{i}\eta\boldsymbol{S}_1 - (\boldsymbol{D}_2 - \mathrm{i}\eta\boldsymbol{S}_2)]\widetilde{\boldsymbol{\psi}} = 2\widetilde{\boldsymbol{g}} \quad \text{on } \mathbb{R}.$$

The remaining part of this section consists of three subsections, which focuses on the singularity analysis of the kernels in the integral operators $\boldsymbol{S}_1, \boldsymbol{D}_1$, and $\boldsymbol{D}_2 - \mathrm{i}\eta\boldsymbol{S}_2$, respectively.

3.1. Separating the logarithmic part of $\boldsymbol{S}_1$

This subsection is devoted to separating the logarithmic part of the operator $\boldsymbol{S}_1$. We first introduce some notations which will be used later. For $\mathbf{x}(s), \mathbf{y}(t) \in \Gamma$, we define the distance between $\mathbf{x}(s)$ and $\mathbf{y}(t)$ as

$$r = r(s,t) := |\mathbf{x}(s) - \mathbf{y}(t)|,$$

and define the upward unit normal at $\mathbf{x}(s)$ and $\mathbf{y}(t)$ as

$$\begin{aligned}
&\boldsymbol{\nu}(s) = \big(\nu_1(s), \nu_2(s)\big)^\top, \quad \nu_1(s) = -\frac{f'(s)}{\sqrt{1+f'(s)^2}}, \quad \nu_2(s) = \frac{1}{\sqrt{1+f'(s)^2}},\\
&\boldsymbol{\nu}(t) = \big(\nu_1(t), \nu_2(t)\big)^\top, \quad \nu_1(t) = -\frac{f'(t)}{\sqrt{1+f'(t)^2}}, \quad \nu_2(t) = \frac{1}{\sqrt{1+f'(t)^2}}.
\end{aligned}$$

Then for convenience, we define the vectors $\boldsymbol{l}$ and $\boldsymbol{l}^\perp$ as

$$\begin{aligned}
&\boldsymbol{l}(s) = \sqrt{1+f'(s)^2}\boldsymbol{\nu}(s), \quad \boldsymbol{l}^\perp(s) = \sqrt{1+f'(s)^2}\boldsymbol{\nu}^\perp(s),\\
&\boldsymbol{l}(t) = \sqrt{1+f'(t)^2}\boldsymbol{\nu}(t), \quad \boldsymbol{l}^\perp(t) = \sqrt{1+f'(t)^2}\boldsymbol{\nu}^\perp(t).
\end{aligned}$$

In terms of (2.7), a direct calculation shows that the Green's tensor $\boldsymbol{\Psi}$ can be represented as

$$\begin{aligned}
\boldsymbol{\Psi}\big(\mathbf{x}(s), \mathbf{y}(t)\big) = &\left[\frac{\mathrm{i}}{4\mu}H_0^{(1)}(\kappa_{\mathrm{s}} r) - \frac{\mathrm{i}}{4\omega^2}\frac{\kappa_{\mathrm{s}}H_1^{(1)}(\kappa_{\mathrm{s}} r) - \kappa_{\mathrm{p}}H_1^{(1)}(\kappa_{\mathrm{p}} r)}{r}\right]\boldsymbol{I}\\
&+ \frac{\mathrm{i}}{4\omega^2}\frac{\kappa_{\mathrm{s}}^2 H_2^{(1)}(\kappa_{\mathrm{s}} r) - \kappa_{\mathrm{p}}^2 H_2^{(1)}(\kappa_{\mathrm{p}} r)}{r^2}\boldsymbol{J}\big(\mathbf{x}(s) - \mathbf{y}(t)\big),
\end{aligned} \tag{3.7}$$

where $\boldsymbol{I}$ is the identity matrix and $\boldsymbol{J}(\mathrm{z}) := \mathrm{z}\mathrm{z}^\top$ for $\mathrm{z} = (z_1, z_2)^\top$. Thus, the operator $\boldsymbol{S}_1$ can be rewritten as

$$(\boldsymbol{S}_1\widetilde{\boldsymbol{\psi}})(s) = \int_{\mathbb{R}} \boldsymbol{A}_1(s,t)\widetilde{\boldsymbol{\psi}}(t)dt, \quad s \in \mathbb{R}$$

with the element of the matrix $\boldsymbol{A}_1(s,t)$ given by

$$\boldsymbol{A}_1(s,t) = 2\boldsymbol{\Psi}\big(x(s), y(t)\big)\sqrt{1+f'(t)^2}.$$

Based on the singularity of $\boldsymbol{A}_1(s,t)$, we can separate the logarithmic part and decompose $\boldsymbol{A}_1(s,t)$ as

$$\boldsymbol{A}_1(s,t) = \boldsymbol{B}_1(s,t)\ln|s-t| + \boldsymbol{C}_1(s,t),$$

where

$$\begin{aligned}
\boldsymbol{B}_1(s,t) = \frac{1}{\pi}\Bigg\{&\left[-\frac{1}{\mu}J_0(\kappa_{\mathrm{s}} r) + \frac{1}{\omega^2}\frac{\kappa_{\mathrm{s}}J_1(\kappa_{\mathrm{s}} r) - \kappa_{\mathrm{p}}J_1(\kappa_{\mathrm{p}} r)}{r}\right]\boldsymbol{I}\\
&- \frac{1}{\omega^2}\frac{\kappa_{\mathrm{s}}^2 J_2(\kappa_{\mathrm{s}} r) - \kappa_{\mathrm{p}}^2 J_2(\kappa_{\mathrm{p}} r)}{r^2}\boldsymbol{J}\big(\mathbf{x}(s) - \mathbf{y}(t)\big)\Bigg\}\sqrt{1+f'(t)^2},
\end{aligned} \tag{3.8}$$

$$\boldsymbol{C}_1(s,t) = \boldsymbol{A}_1(s,t) - \boldsymbol{B}_1(s,t)\ln|s-t|. \tag{3.9}$$

To get the exact expressions of $\boldsymbol{B}_1(s,t)$ and $\boldsymbol{C}_1(s,t)$ while $s = t$ for numerical computation, we need to introduce the definitions of Bessel functions J_n and Neumann functions Y_n (see [14,

Eqs. (3.97), (3.98)]), which are given by

$$J_n(r) := \sum_{p=0}^{\infty} \frac{(-1)^p}{p!(n+p)!} \left(\frac{r}{2}\right)^{n+2p}, \tag{3.10}$$

$$Y_n(r) := \frac{2}{\pi}\left\{\ln\frac{r}{2} + C_E\right\} J_n(r) - \frac{1}{\pi}\sum_{p=0}^{n-1} \frac{(n-1-p)!}{p!}\left(\frac{2}{r}\right)^{n-2p} - \frac{1}{\pi}\sum_{p=0}^{\infty} \frac{(-1)^p}{p!(n+p)!}\left(\frac{r}{2}\right)^{n+2p} \{\phi(p+n)+\phi(p)\} \tag{3.11}$$

for $n = 0, 1, 2, \ldots$, and $r \in (0, \infty)$. Here, C_E denotes Euler's constant, and for $n = 0$ the finite sum in (3.11) is set equal to zero, and the function ϕ is defined by

$$\phi(0) = 0 \quad \text{and} \quad \phi(p) := \sum_{m=1}^{p} \frac{1}{m}, \quad p = 1, 2, \ldots .$$

Let

$$L_n(r) := H_n^{(1)}(r) - \frac{2\mathrm{i}}{\pi} J_n(r)\ln(r)$$

for $n = 0, 1, 2, \ldots$, then with the aid of $H_n^{(1)}(r) = J_n(r) + \mathrm{i}Y_n(r)$ and (3.10)-(3.11), we can derive the following limits:

$$\lim_{r\to 0} L_0(\kappa_{\mathrm{s}} r) = \alpha_1, \tag{3.12}$$

$$\lim_{r\to 0}\left\{\frac{\kappa_{\mathrm{s}}}{r} L_1(\kappa_{\mathrm{s}} r) + \frac{2\mathrm{i}}{\pi r^2}\right\} = \frac{1}{2}\kappa_{\mathrm{s}}^2\left(\alpha_1 - \frac{\mathrm{i}}{\pi}\right), \tag{3.13}$$

$$\lim_{r\to 0}\frac{\kappa_{\mathrm{s}} L_1(\kappa_{\mathrm{s}} r) - \kappa_{\mathrm{p}} L_1(\kappa_{\mathrm{p}} r)}{r} = \frac{1}{2}\alpha_2\left(\alpha_1 - \frac{\mathrm{i}}{\pi}\right), \tag{3.14}$$

$$\lim_{r\to 0}\left\{\frac{\kappa_{\mathrm{s}}^2 L_2(\kappa_{\mathrm{s}} r) - \kappa_{\mathrm{p}}^2 L_2(\kappa_{\mathrm{p}} r)}{r^2} + \frac{\mathrm{i}\alpha_2}{\pi r^2}\right\} = \frac{1}{8}\alpha_3\left(\alpha_1 - \frac{3\mathrm{i}}{2\pi}\right), \tag{3.15}$$

$$\lim_{r\to 0}\left\{\frac{\kappa_{\mathrm{s}}^3 L_3(\kappa_{\mathrm{s}} r) - \kappa_{\mathrm{p}}^3 L_3(\kappa_{\mathrm{p}} r)}{r^3} + \frac{2\mathrm{i}\alpha_2}{\pi r^4} + \frac{\mathrm{i}\alpha_3}{4\pi r^2}\right\} = \frac{1}{48}\alpha_4\left(\alpha_1 - \frac{11\mathrm{i}}{6\pi}\right), \tag{3.16}$$

where the constants $\alpha_j, j = 1, 2, 3, 4$, are defined by

$$\alpha_1 := 1 + \frac{2\mathrm{i}}{\pi}(C_E - \ln 2), \quad \alpha_2 := \kappa_{\mathrm{s}}^2 - \kappa_{\mathrm{p}}^2, \quad \alpha_3 := \kappa_{\mathrm{s}}^4 - \kappa_{\mathrm{p}}^4, \quad \alpha_4 := \kappa_{\mathrm{s}}^6 - \kappa_{\mathrm{p}}^6.$$

With the help of (3.12)-(3.15), we can derive the diagonal terms

$$\boldsymbol{B}_1(s,s) = \frac{1}{\pi}\left(-\frac{1}{\mu} + \frac{\alpha_5}{2}\right)\sqrt{1+f'(s)^2}\,\boldsymbol{I}, \tag{3.17}$$

$$\boldsymbol{C}_1(s,s) = \left\{\left[\frac{\mathrm{i}}{4}\alpha_1\alpha_6 - \frac{\alpha_5}{4\pi} - \frac{1}{2\pi}\left(c_{\mathrm{s}}^2 \ln\left(\kappa_{\mathrm{s}}\sqrt{1+f'(s)^2}\right) + c_{\mathrm{p}}^2 \ln\left(\kappa_{\mathrm{p}}\sqrt{1+f'(s)^2}\right)\right)\right]\boldsymbol{I} + \frac{\alpha_5}{2\pi}\frac{\boldsymbol{J}\big(\boldsymbol{l}^{\perp}(s)\big)}{1+f'(s)^2}\right\}\sqrt{1+f'(s)^2}, \tag{3.18}$$

where the constants $\alpha_j, j = 5, 6$, are defined by $\alpha_5 := c_{\mathrm{s}}^2 - c_{\mathrm{p}}^2$ and $\alpha_6 := c_{\mathrm{s}}^2 + c_{\mathrm{p}}^2$.

3.2. Separating the logarithmic part of $\boldsymbol{D}_1$

The purpose of this subsection is to separate the logarithmic part of the operator $\boldsymbol{D}_1$. Due to (3.2), (3.6), (2.3) and (3.7), we can write $\boldsymbol{D}_1$ as

$$(\boldsymbol{D}_1\widetilde{\boldsymbol{\psi}})(s)=\int_{\mathbb{R}}\boldsymbol{A}_2(s,t)\widetilde{\boldsymbol{\psi}}(t)dt,\quad s\in\mathbb{R}.$$

Here, a direct calculation shows that the matrix $\boldsymbol{A}_2(s,t)$ is given by

$$\begin{aligned}\boldsymbol{A}_2(s,t)=(\mu+\widetilde{\mu})\Bigg\{&\Bigg[-\frac{\mathrm{i}}{2\mu}\frac{\kappa_{\mathrm{s}}H_1^{(1)}(\kappa_{\mathrm{s}}r)}{r}+\frac{\mathrm{i}}{2\omega^2}\frac{\kappa_{\mathrm{s}}^2H_2^{(1)}(\kappa_{\mathrm{s}}r)-\kappa_{\mathrm{p}}^2H_2^{(1)}(\kappa_{\mathrm{p}}r)}{r^2}\Bigg]\boldsymbol{I}\\&-\frac{\mathrm{i}}{2\omega^2}\frac{\kappa_{\mathrm{s}}^3H_3^{(1)}(\kappa_{\mathrm{s}}r)-\kappa_{\mathrm{p}}^3H_3^{(1)}(\kappa_{\mathrm{p}}r)}{r^3}\boldsymbol{J}\big(\mathbf{x}(s)-\mathbf{y}(t)\big)\Bigg\}\big[(s-t)f'(t)+f(t)-f(s)\big]\\&-(\mu+\widetilde{\mu})\frac{\mathrm{i}}{2\omega^2}\frac{\kappa_{\mathrm{s}}^2H_2^{(1)}(\kappa_{\mathrm{s}}r)-\kappa_{\mathrm{p}}^2H_2^{(1)}(\kappa_{\mathrm{p}}r)}{r^2}\boldsymbol{M}_1(s,t)\\&+\widetilde{\lambda}\Bigg[\frac{\mathrm{i}}{2\mu}\frac{\kappa_{\mathrm{s}}H_1^{(1)}(\kappa_{\mathrm{s}}r)}{r}-\frac{2\mathrm{i}}{\omega^2}\frac{\kappa_{\mathrm{s}}^2H_2^{(1)}(\kappa_{\mathrm{s}}r)-\kappa_{\mathrm{p}}^2H_2^{(1)}(\kappa_{\mathrm{p}}r)}{r^2}\\&\quad+\frac{\mathrm{i}}{2\omega^2}\frac{\kappa_{\mathrm{s}}^3H_3^{(1)}(\kappa_{\mathrm{s}}r)-\kappa_{\mathrm{p}}^3H_3^{(1)}(\kappa_{\mathrm{p}}r)}{r}\Bigg]\boldsymbol{M}_2(s,t)-\widetilde{\mu}\frac{\mathrm{i}}{2\mu}\frac{\kappa_{\mathrm{s}}H_1^{(1)}(\kappa_{\mathrm{s}}r)}{r}\boldsymbol{M}_3(s,t)\end{aligned}$$

with

$$\begin{aligned}\boldsymbol{M}_1(s,t)&:=\big(\mathbf{x}(s)-\mathbf{y}(t)\big)\boldsymbol{l}(t)^\top+\boldsymbol{l}(t)\big(\mathbf{x}(s)-\mathbf{y}(t)\big)^\top,\\\boldsymbol{M}_2(s,t)&:=\big(\mathbf{x}(s)-\mathbf{y}(t)\big)\boldsymbol{l}(t)^\top,\\\boldsymbol{M}_3(s,t)&:=\big(\mathbf{x}(s)-\mathbf{y}(t)\big)^\perp\boldsymbol{l}^\perp(t)^\top.\end{aligned}$$

Based on the singularity of $\boldsymbol{A}_2(s,t)$, we can separate the logarithmic part of $\boldsymbol{A}_2(s,t)$ as

$$\boldsymbol{A}_2(s,t)=\boldsymbol{B}_2(s,t)\ln|s-t|+\boldsymbol{C}_2(s,t),$$

where

$$\begin{aligned}\boldsymbol{B}_2(s,t):=(\mu+\widetilde{\mu})\Bigg\{&\Bigg[\frac{1}{\pi\mu}\frac{\kappa_{\mathrm{s}}J_1(\kappa_{\mathrm{s}}r)}{r}-\frac{1}{\pi\omega^2}\frac{\kappa_{\mathrm{s}}^2J_2(\kappa_{\mathrm{s}}r)-\kappa_{\mathrm{p}}^2J_2(\kappa_{\mathrm{p}}r)}{r^2}\Bigg]\boldsymbol{I}\\&+\frac{1}{\pi\omega^2}\frac{\kappa_{\mathrm{s}}^3J_3(\kappa_{\mathrm{s}}r)-\kappa_{\mathrm{p}}^3J_3(\kappa_{\mathrm{p}}r)}{r^3}\boldsymbol{J}\big(\mathbf{x}(s)-\mathbf{y}(t)\big)\Bigg\}\big[(s-t)f'(t)+f(t)-f(s)\big]\\&+(\mu+\widetilde{\mu})\frac{1}{\pi\omega^2}\frac{\kappa_{\mathrm{s}}^2J_2(\kappa_{\mathrm{s}}r)-\kappa_{\mathrm{p}}^2J_2(\kappa_{\mathrm{p}}r)}{r^2}\boldsymbol{M}_1(s,t)\\&+\widetilde{\lambda}\Bigg[-\frac{1}{\pi\mu}\frac{\kappa_{\mathrm{s}}J_1(\kappa_{\mathrm{s}}r)}{r}+\frac{4}{\pi\omega^2}\frac{\kappa_{\mathrm{s}}^2J_2(\kappa_{\mathrm{s}}r)-\kappa_{\mathrm{p}}^2J_2(\kappa_{\mathrm{p}}r)}{r^2}\\&\quad-\frac{1}{\pi\omega^2}\frac{\kappa_{\mathrm{s}}^3J_3(\kappa_{\mathrm{s}}r)-\kappa_{\mathrm{p}}^3J_3(\kappa_{\mathrm{p}}r)}{r}\Bigg]\boldsymbol{M}_2(s,t)+\widetilde{\mu}\frac{1}{\pi\mu}\frac{\kappa_{\mathrm{s}}J_1(\kappa_{\mathrm{s}}r)}{r}\boldsymbol{M}_3(s,t),\end{aligned}\tag{3.19}$$

$$\boldsymbol{C}_2(s,t):=\boldsymbol{A}_2(s,t)-\boldsymbol{B}_2(s,t)\ln|s-t|.\tag{3.20}$$

Similar to the previous subsection, we need to get the exact expressions of $\boldsymbol{B}_2(s,t)$ and $\boldsymbol{C}_2(s,t)$ while $s=t$ for numerical computation. Using Eqs. (3.13), (3.15) and (3.16), choosing $\widetilde{\mu}$ as in (2.10) and by a direct but lengthy calculation we obtain the diagonal terms

$$\boldsymbol{B}_2(s,s)=0, \tag{3.21}$$

$$\boldsymbol{C}_2(s,s)=-\frac{1}{2\pi}\frac{f''(s)}{1+f'(s)^2}\left\{\left[-1+\frac{\mu+\widetilde{\mu}}{2}\alpha_5\right]\boldsymbol{I}-\alpha_5(\mu+\widetilde{\mu})\frac{\boldsymbol{J}\big(\boldsymbol{l}^{\perp}(s)\big)}{1+f'(s)^2}\right\}. \tag{3.22}$$

3.3. The computation of $\boldsymbol{D}_2-\mathrm{i}\eta\boldsymbol{S}_2$

Observing from (3.3), (3.5), and (3.6), the kernel of the integral operator $\boldsymbol{D}_2-\mathrm{i}\eta\boldsymbol{S}_2$ is related to $\boldsymbol{\Psi}(\mathbf{x},\mathbf{y}')$ and $\boldsymbol{U}(\mathbf{x},\mathbf{y})$ with $\mathbf{x}=(s,f(s))\in\Gamma$, $\mathbf{y}=(t,f(t))\in\Gamma$, and $\mathbf{y}'=(t,2h-f(t))$. Due to $h<\inf_{\mathrm{x}_1\in\mathbb{R}}f(\mathrm{x}_1)$, it is readily seen that there is a positive distance between $\mathbf{x}$ and $\mathbf{y}'$, which leads to that $\boldsymbol{\Psi}(\mathbf{x},\mathbf{y}')$ is smooth, and by [3, Theorem 2.1], we have $\boldsymbol{U}(\mathbf{x},\mathbf{y})\in[C^{\infty}(U_h)\cap C^1(\overline{U_h})]^{2\times2}$. It follows from (3.3), (3.5), (3.6), (2.3), (2.7) and a direct but lengthy calculation that the integral operator $\boldsymbol{D}_2-\mathrm{i}\eta\boldsymbol{S}_2$ can be rewritten as integral on the real line, which reads

$$\left[(\boldsymbol{D}_2-\mathrm{i}\eta\boldsymbol{S}_2)\widetilde{\boldsymbol{\psi}}\right](s)=\int_{\mathbb{R}}\boldsymbol{A}_3(s,t)\widetilde{\boldsymbol{\psi}}(t)dt,\quad s\in\mathbb{R},$$

where

$$\boldsymbol{A}_3(s,t)=\boldsymbol{A}_4(s,t)-\boldsymbol{A}_5(s,t) \tag{3.23}$$

with

$$\begin{aligned}\boldsymbol{A}_4(s,t)&:=2\big[\boldsymbol{P}^{(\mathbf{y})}\boldsymbol{\Psi}(\mathbf{x},\mathbf{y}')-\mathrm{i}\eta\boldsymbol{\Psi}(\mathbf{x},\mathbf{y}')\big]\sqrt{1+f'(t)^2}\\&=:\boldsymbol{A}_{41}+\boldsymbol{A}_{42}+\boldsymbol{A}_{43}+\boldsymbol{A}_{44},\\\boldsymbol{A}_5(s,t)&:=2\big[\boldsymbol{P}^{(\mathbf{y})}\boldsymbol{U}(\mathbf{x},\mathbf{y})-\mathrm{i}\eta\boldsymbol{U}(\mathbf{x},\mathbf{y})\big]\sqrt{1+f'(t)^2}.\end{aligned}$$

Here, $\boldsymbol{A}_{4j},j=1,2,3,4$, are defined by

$$\begin{aligned}\boldsymbol{A}_{41}=(\mu+\widetilde{\mu})\Bigg\{\Bigg[&-\frac{\mathrm{i}}{2\mu}\frac{\kappa_{\mathrm{s}}H_1^{(1)}(\kappa_{\mathrm{s}}r')}{r'}\boldsymbol{I}+\frac{\mathrm{i}}{2\omega^2}\frac{\kappa_{\mathrm{s}}^2H_2^{(1)}(\kappa_{\mathrm{s}}r')-\kappa_{\mathrm{p}}^2H_2^{(1)}(\kappa_{\mathrm{p}}r')}{r'^2}\boldsymbol{I}\\&-\frac{\mathrm{i}}{2\omega^2}\frac{\kappa_{\mathrm{s}}^3H_3^{(1)}(\kappa_{\mathrm{s}}r')-\kappa_{\mathrm{p}}^3H_3^{(1)}(\kappa_{\mathrm{p}}r')}{r'^3}\boldsymbol{J}\big(\mathbf{x}(s)-\mathbf{y}'(t)\big)\Bigg]\\&\times[(s-t)f'(t)+f(t)+f(s)-2h]\\&+\frac{\mathrm{i}}{2\omega^2}\frac{\kappa_{\mathrm{s}}^2H_2^{(1)}(\kappa_{\mathrm{s}}r')-\kappa_{\mathrm{p}}^2H_2^{(1)}(\kappa_{\mathrm{p}}r')}{r'^2}\boldsymbol{M}_4(s,t)\Bigg\},\end{aligned}$$

$$\begin{aligned}\boldsymbol{A}_{42}=\widetilde{\lambda}\Bigg\{\Bigg[&-\frac{\mathrm{i}}{2\mu}\frac{\kappa_{\mathrm{s}}H_1^{(1)}(\kappa_{\mathrm{s}}r')}{r'}+\frac{\mathrm{i}}{\omega^2}\frac{\kappa_{\mathrm{s}}^2H_2^{(1)}(\kappa_{\mathrm{s}}r')-\kappa_{\mathrm{p}}^2H_2^{(1)}(\kappa_{\mathrm{p}}r')}{r'^2}\Bigg]\boldsymbol{Q}\\&+\frac{\mathrm{i}}{2\omega^2}\frac{\kappa_{\mathrm{s}}^3H_3^{(1)}(\kappa_{\mathrm{s}}r')-\kappa_{\mathrm{p}}^3H_3^{(1)}(\kappa_{\mathrm{p}}r')}{r'^3}\big[(t-s)^2-\big(f(t)+f(s)-2h\big)^2\big]\boldsymbol{I}\Bigg\}\boldsymbol{M}_5(s,t),\end{aligned}$$

$$\boldsymbol{A}_{43}=-\widetilde{\mu}\Bigg\{\Bigg[-\frac{\mathrm{i}}{2\mu}\frac{\kappa_{\mathrm{s}}H_1^{(1)}(\kappa_{\mathrm{s}}r')}{r'}+\frac{\mathrm{i}}{\omega^2}\frac{\kappa_{\mathrm{s}}^2H_2^{(1)}(\kappa_{\mathrm{s}}r')-\kappa_{\mathrm{p}}^2H_2^{(1)}(\kappa_{\mathrm{p}}r')}{r'^2}\Bigg]\boldsymbol{M}_6(s,t)$$

$$-\frac{\mathrm{i}}{\omega^2}\frac{\kappa_{\mathrm{s}}^3 H_3^{(1)}(\kappa_{\mathrm{s}}r') - \kappa_{\mathrm{p}}^3 H_3^{(1)}(\kappa_{\mathrm{p}}r')}{r'^3}(s-t)\big(f(s)+f(t)-2h\big)\boldsymbol{M}_7(s,t)\Bigg\},$$

$$\boldsymbol{A}_{44} = \eta\Bigg\{\left[\frac{1}{2\mu}H_0^{(1)}(\kappa_{\mathrm{s}}r') - \frac{1}{2\omega^2}\frac{\kappa_{\mathrm{s}}H_1^{(1)}(\kappa_{\mathrm{s}}r') - \kappa_{\mathrm{p}}H_1^{(1)}(\kappa_{\mathrm{p}}r')}{r'}\right]\boldsymbol{I}$$
$$+\frac{1}{2\omega^2}\frac{\kappa_{\mathrm{s}}^2 H_2^{(1)}(\kappa_{\mathrm{s}}r') - \kappa_{\mathrm{p}}^2 H_2^{(1)}(\kappa_{\mathrm{p}}r')}{r'^2}\boldsymbol{J}\big(\mathbf{x}(s)-\mathbf{y}'(t)\big)\Bigg\}\sqrt{1+f'(t)^2},$$

where $r' = r'(s,t) := |\mathbf{x}(s)-\mathbf{y}'(t)|$ denotes the distance between $\mathbf{x}$ and $\mathbf{y}'$, $\boldsymbol{Q} = \mathrm{diag}(-1,1)$ and

$$\begin{aligned}
&\boldsymbol{M}_{4,jk}(s,t) := \big(\mathrm{x}_k(s)-\mathrm{y}_k'(t)\big)q_j l_j(t) + \big(\mathrm{x}_j(s)-\mathrm{y}_j'(t)\big)q_k l_k(t),\\
&\boldsymbol{M}_5(s,t) := \big(\mathbf{x}(s)-\mathbf{y}'(t)\big)\boldsymbol{l}(t)^\top,\\
&\boldsymbol{M}_{6,jk}(s,t) := \big[(s-t)\delta_{j2} + \big(f(s)+f(t)-2h\big)\delta_{j1}\big]l_k^\perp(t),\\
&\boldsymbol{M}_7(s,t) := \big(\mathbf{x}(s)-\mathbf{y}'(t)\big)\boldsymbol{l}^\perp(t)^\top
\end{aligned}$$

with the vector $\boldsymbol{q} = (-1,1)^\top$ and δ_{jk} being the Kronecker delta function satisfying $\delta_{jk} = 1$ for $j = k$ and $\delta_{jk} = 0$ for $j \neq k$.

According to the above three subsections on the analysis of $\boldsymbol{S}_1, \boldsymbol{D}_1$, and $\boldsymbol{D}_2 - \mathrm{i}\eta\boldsymbol{S}_2$, the integral operator $\boldsymbol{D} - \mathrm{i}\eta\boldsymbol{S}$ can be rewritten in the following form:

$$\Big[(\boldsymbol{D}-\mathrm{i}\eta\boldsymbol{S})\widetilde{\boldsymbol{\psi}}\Big](s) = \int_{\mathbb{R}} \boldsymbol{A}(s,t)\widetilde{\boldsymbol{\psi}}(t)dt \tag{3.24}$$

with

$$\boldsymbol{A}(s,t) = -\mathrm{i}\eta\boldsymbol{A}_1(s,t) + \boldsymbol{A}_2(s,t) - \boldsymbol{A}_3(s,t) := \boldsymbol{B}^*(s,t)\ln|s-t| + \boldsymbol{C}^*(s,t),$$

where $\boldsymbol{B}^*(s,t)$ and $\boldsymbol{C}^*(s,t)$ are

$$\boldsymbol{B}^*(s,t) := -\mathrm{i}\eta\boldsymbol{B}_1(s,t) + \boldsymbol{B}_2(s,t), \tag{3.25}$$
$$\boldsymbol{C}^*(s,t) := -\mathrm{i}\eta\boldsymbol{C}_1(s,t) + \boldsymbol{C}_2(s,t) - \boldsymbol{A}_3(s,t). \tag{3.26}$$

In order to employ the Nyström method, we follow the ideas of [25, Theorem 2.1] and rewrite the integral kernel $\boldsymbol{A}(s,t)$ in the form (3.1) with $\boldsymbol{B}(s,t)$ and $\boldsymbol{C}(s,t)$ given by

$$\boldsymbol{B}(s,t) := \pi\boldsymbol{B}^*(s,t)\chi(s-t), \tag{3.27}$$
$$\boldsymbol{C}(s,t) := \boldsymbol{B}^*(s,t)\left[\big(1-\chi(s-t)\big)\ln|s-t| - \chi(s-t)\ln\left(\frac{\sin\big((s-t)/2\big)}{(s-t)/2}\right)\right] + \boldsymbol{C}^*(s,t) \tag{3.28}$$

for $s \neq t$, where $\chi \in C_0^\infty(\mathbb{R})$ is a cut-off function defined by

$$\chi(s) = \begin{cases} 1, & |s| \le 1,\\ \left[1+\exp\left(\dfrac{1}{\pi-|s|}+\dfrac{1}{1-|s|}\right)\right]^{-1}, & 1<|s|<\pi,\\ 0, & \pi \le |s|. \end{cases}$$

Finally, with the help of (3.17), (3.18), (3.21), (3.22), (3.27) and (3.28), we obtain that

$$\begin{aligned}
&\boldsymbol{B}(s,s) := \pi[-\mathrm{i}\eta\boldsymbol{B}_1(s,s) + \boldsymbol{B}_2(s,s)],\\
&\boldsymbol{C}(s,s) := -\mathrm{i}\eta\boldsymbol{C}_1(s,s) + \boldsymbol{C}_2(s,s) - \boldsymbol{A}_3(s,s).
\end{aligned}$$

4. Convergence Analysis of the Nyström Method

The goal of this section is to establish the convergence result of the Nyström method for the boundary integral equation (2.15). In views of (3.24), (2.15) can be rewritten in the following form:

$$\widetilde{\boldsymbol{\psi}}(s)+\frac{1}{2\pi}\int_{-\infty}^{+\infty}\ln\left(4\sin^2\frac{s-t}{2}\right)\boldsymbol{B}(s,t)\widetilde{\boldsymbol{\psi}}(t)dt+\int_{-\infty}^{+\infty}\boldsymbol{C}(s,t)\widetilde{\boldsymbol{\psi}}(t)dt=2\widetilde{\boldsymbol{g}}(s),\quad s\in\mathbb{R}.\tag{4.1}$$

To get the numerical solution of (4.1), we truncate the infinite interval $(-\infty,+\infty)$ into a finite interval $(-R,R)$, and choose an equidistant set of knots $t_j:=-R+j\pi/N$ for $j=0,1,\ldots,2NR/\pi$. If $\boldsymbol{B}(s,t)\in C^n_{0,\pi}(\mathbb{R}^2)$ and $\boldsymbol{C}(s,t)\in BC^n_p(\mathbb{R}^2)$ for some $p>1$ and some positive integer n, it follows from [25] that the two integrals in (4.1) can be approximated by

$$\begin{aligned}&\frac{1}{2\pi}\int_{-\infty}^{+\infty}\ln\left(4\sin^2\frac{s-t}{2}\right)\boldsymbol{B}(s,t)\widetilde{\boldsymbol{\psi}}(t)dt\approx\sum_{j\in\mathbb{Z}}R_j^{(N)}(s)\boldsymbol{B}(s,t_j)\widetilde{\boldsymbol{\psi}}(t_j),\quad s\in\mathbb{R},\\&\int_{-\infty}^{+\infty}\boldsymbol{C}(s,t)\widetilde{\boldsymbol{\psi}}(t)dt\approx\frac{\pi}{N}\sum_{j\in\mathbb{Z}}\boldsymbol{C}(s,t_j)\widetilde{\boldsymbol{\psi}}(t_j),\qquad\qquad s\in\mathbb{R}\end{aligned}$$

with the quadrature weights given by

$$R_j^{(N)}(s):=-\frac{1}{N}\left[\sum_{m=1}^{N-1}\frac{1}{m}\cos m(s-t_j)+\frac{1}{2N}\cos N(s-t_j)\right].$$

Therefore, an approximated form of (4.1) is

$$\widetilde{\boldsymbol{\psi}}_N(s)+\sum_{j\in\mathbb{Z}}\alpha_j^{(N)}(s)\widetilde{\boldsymbol{\psi}}_N(t_j)=2\widetilde{\boldsymbol{g}}(s),\quad s\in\mathbb{R}\tag{4.2}$$

with

$$\alpha_j^{(N)}(s):=R_j^{(N)}(s)\boldsymbol{B}(s,t_j)+\frac{\pi}{N}\boldsymbol{C}(s,t_j).$$

The remaining part of this section is to study the convergence result for $\|\widetilde{\boldsymbol{\psi}}-\widetilde{\boldsymbol{\psi}}_N\|_{[L^\infty(\mathbb{R})]^2}$, which is presented in the following theorem.

Theorem 4.1. *Let $f\in B^{(n+2)}_{c_1,c_2}$ and $\widetilde{\boldsymbol{g}}\in[BC^n(\mathbb{R})]^2$ for some $n\in\mathbb{N}$ and $c_1,c_2>0$. There exists $N_0\in\mathbb{N}$ such that (4.2) admits a uniquely determined numerical solution $\widetilde{\boldsymbol{\psi}}_N$ and*

$$\left\|\widetilde{\boldsymbol{\psi}}-\widetilde{\boldsymbol{\psi}}_N\right\|_{[L^\infty(\mathbb{R})]^2}\lesssim N^{-n}\|\widetilde{\boldsymbol{g}}\|_{[BC^n(\mathbb{R})]^2}$$

for $N>N_0$, where $\widetilde{\boldsymbol{\psi}}$ is the unique solution of (2.15).

Proof. According to Theorem 2.2, the integral equation (2.15) has exactly one solution $\widetilde{\boldsymbol{\psi}}\in[BC(\mathbb{R})]^2$ for every $\widetilde{\boldsymbol{g}}\in[BC(\mathbb{R})]^2$ and there exists $C_0>0$ such that $\|(\boldsymbol{I}+\boldsymbol{D}-\mathrm{i}\eta\boldsymbol{S})^{-1}\|\le C_0$. Then by [25, Theorem 3.13], the statement of this theorem holds if $\boldsymbol{B}(s,t)\in[C^n_{0,\pi}(\mathbb{R}^2)]^{2\times2}$ and $\boldsymbol{C}(s,t)\in[BC^n_p(\mathbb{R}^2)]^{2\times2}$ for some $p>1$. With the help of [25, Theorem 2.1], it is equivalent to showing the following three conditions: For all $j,k\in\mathbb{N}$ with $j+k\le n$, there exists constants $C>0$ and $p>1$ such that

$$\textbf{C1}. \quad \left|\frac{\partial^{j+k}\boldsymbol{B}^*(s,t)}{\partial s^j\partial t^k}\right| \le C, \qquad s,t\in\mathbb{R}, \quad |s-t|\le\pi,$$

$$\textbf{C2}. \quad \left|\frac{\partial^{j+k}\boldsymbol{C}^*(s,t)}{\partial s^j\partial t^k}\right| \le C, \qquad s,t\in\mathbb{R}, \quad |s-t|\le\pi,$$

$$\textbf{C3}. \quad \left|\frac{\partial^{j+k}\boldsymbol{A}(s,t)}{\partial s^j\partial t^k}\right| \le C\,(1+|s-t|)^{-p}, \quad s,t\in\mathbb{R}, \quad |s-t|\ge\pi,$$

where $\boldsymbol{B}^*(s,t)$ and $\boldsymbol{C}^*(s,t)$ are defined by (3.25) and (3.26), respectively. Thus, it suffices to show that **C1**-**C3** hold.

For the condition **C1**, we recall that

$$\boldsymbol{B}^*(s,t) = -\mathrm{i}\eta\boldsymbol{B}_1(s,t) + \boldsymbol{B}_2(s,t),$$

where $\boldsymbol{B}_1(s,t)$ and $\boldsymbol{B}_2(s,t)$ are defined by (3.8) and (3.19), respectively. By (3.10) and the fact that $J_n(r)$ is analytic for all $r\in\mathbb{R}$, we obtain that $J_n(r)/r^n$ is also analytic for all $r\in\mathbb{R}$. Since $f\in B^{(n+2)}_{c_1,c_2}$, it follows from (3.8) and (3.19) that $\boldsymbol{B}_1(s,t)\in[BC^n(\mathbb{R}^2)]^{2\times2}$ and $\boldsymbol{B}_2(s,t)\in[BC^n(\mathbb{R}^2)]^{2\times2}$, which implies that **C1** holds.

For the condition **C2**, we recall that

$$\boldsymbol{C}^*(s,t) = -\mathrm{i}\eta\boldsymbol{C}_1(s,t) + \boldsymbol{C}_2(s,t) - \boldsymbol{A}_3(s,t),$$

where $\boldsymbol{C}_1(s,t), \boldsymbol{C}_2(s,t)$, and $\boldsymbol{A}_3(s,t)$ are defined by (3.9), (3.20), and (3.23), respectively. To prove this condition, we first introduce the following notations:

$$\begin{aligned}
&\rho_n(\kappa,s,t) := H_n^{(1)}(\kappa r) - \frac{2\mathrm{i}}{\pi}J_n(\kappa r)\ln|s-t|,\\
&\gamma_1(s,t) := \frac{1}{r}\big(\kappa_{\mathrm{s}}\rho_1(\kappa_{\mathrm{s}},s,t) - \kappa_{\mathrm{p}}\rho_1(\kappa_{\mathrm{p}},s,t)\big),\\
&\gamma_2(s,t) := \kappa_{\mathrm{s}}^2\rho_2(\kappa_{\mathrm{s}},s,t) - \kappa_{\mathrm{p}}^2\rho_2(\kappa_{\mathrm{p}},s,t),\\
&\gamma_3(s,t) := r\left[\kappa_{\mathrm{s}}^3\rho_3(\kappa_{\mathrm{s}},s,t) - \kappa_{\mathrm{p}}^3\rho_3(\kappa_{\mathrm{p}},s,t)\right],\\
&\xi(s,t) := \frac{1}{r^2}\big((s-t)f'(t) + f(t) - f(s)\big),\\
&F(\kappa,s,t) := 1 + \frac{2\mathrm{i}}{\pi}C_E + \frac{2\mathrm{i}}{\pi}\ln\frac{\kappa r}{2|s-t|},
\end{aligned}$$

and

$$\begin{aligned}
\boldsymbol{Z}_1(s,t) &:= \frac{\boldsymbol{J}\big(\mathbf{x}(s)-\mathbf{y}(t)\big)}{r^2},\\
\boldsymbol{Z}_2(s,t) &:= -(\mu+\widetilde{\mu})\frac{\mathrm{i}}{2\omega^2}\frac{\gamma_2(s,t)}{r^2}\boldsymbol{M}_1(s,t) - \widetilde{\mu}\frac{\mathrm{i}}{2\mu}\frac{\kappa_s}{r}\rho_1(\kappa_{\mathrm{s}},s,t)\boldsymbol{M}_3(s,t)\\
&\quad + \widetilde{\lambda}\left[\frac{\mathrm{i}}{2\mu}\frac{\kappa_{\mathrm{s}}}{r}\rho_1(\kappa_{\mathrm{s}},s,t) - \frac{2\mathrm{i}}{\omega^2}\frac{\gamma_2(s,t)}{r^2} + \frac{\mathrm{i}}{2\omega^2}\frac{\gamma_3(s,t)}{r^2}\right]\boldsymbol{M}_2(s,t).
\end{aligned}$$

Using these notations and (3.26), (3.9) and (3.20), we can rewrite the elements of $\boldsymbol{C}^*(s,t)$ as

$$\begin{aligned}
C^*(s,t) &= -\mathrm{i}\eta\left\{\left[\frac{\mathrm{i}}{2\mu}\rho_0(\kappa_{\mathrm{s}},s,t) - \frac{\mathrm{i}}{2\omega^2}\gamma_1(s,t)\right]\boldsymbol{I} + \frac{\mathrm{i}}{2\omega^2}\gamma_2(s,t)\boldsymbol{Z}_1(s,t)\right\}\sqrt{1+f'(t)^2}\\
&\quad + (\mu+\widetilde{\mu})\left\{\left[-\frac{\mathrm{i}}{2\mu}\kappa_{\mathrm{s}}r\rho_1(\kappa_{\mathrm{s}},s,t) + \frac{\mathrm{i}}{2\omega^2}\gamma_2(s,t)\right]\boldsymbol{I} - \frac{\mathrm{i}}{2\omega^2}\gamma_3(s,t)\boldsymbol{Z}_1(s,t)\right\}\xi(s,t)\\
&\quad + \boldsymbol{Z}_2(s,t) - \boldsymbol{A}_3(s,t). \qquad (4.3)
\end{aligned}$$

With the help of $H_n^{(1)}(z) = J_n(z) + \mathrm{i}Y_n(z)$ and (3.10)-(3.11), we obtain that

$$\rho_0(\kappa, s, t) = F(\kappa, s, t)J_0(\kappa r) - \frac{2\mathrm{i}}{\pi}\sum_{p=0}^{+\infty}\frac{(-1)^p}{(p!)^2}\Big(\frac{\kappa r}{2}\Big)^{2p}\phi(p), \tag{4.4}$$

$$\kappa_{\mathrm{s}} r\rho_1(\kappa_{\mathrm{s}}, s, t) = F(\kappa_{\mathrm{s}}, s, t)\kappa_{\mathrm{s}} rJ_1(\kappa_{\mathrm{s}} r) - \frac{2\mathrm{i}}{\pi} - \frac{2\mathrm{i}}{\pi}\sum_{p=0}^{+\infty}\frac{(-1)^p}{p!(p+1)!}\Big(\frac{\kappa_{\mathrm{s}} r}{2}\Big)^{2+2p}\big(\phi(p+1)+\phi(p)\big), \tag{4.5}$$

$$\gamma_1(s,t) = \kappa_{\mathrm{s}}F(\kappa_{\mathrm{s}}, s, t)\frac{J_1(\kappa_{\mathrm{s}} r)}{r} - \kappa_{\mathrm{p}}F(\kappa_{\mathrm{p}}, s, t)\frac{J_1(\kappa_{\mathrm{p}} r)}{r} - \frac{\mathrm{i}}{2\pi}\sum_{p=0}^{+\infty}\frac{(-1)^p}{p!(p+1)!}\Big(\frac{r}{2}\Big)^{2p}\big(\kappa_{\mathrm{s}}^{2+2p} - \kappa_{\mathrm{p}}^{2+2p}\big)\big(\phi(p)+\phi(p+1)\big), \tag{4.6}$$

$$\gamma_2(s,t) = \kappa_{\mathrm{s}}^2F(\kappa_{\mathrm{s}}, s, t)J_2(\kappa_{\mathrm{s}} r) - \kappa_{\mathrm{p}}^2F(\kappa_{\mathrm{p}}, s, t)J_2(\kappa_{\mathrm{p}} r) - \frac{\mathrm{i}}{\pi}\alpha_2 - \frac{\mathrm{i}}{\pi}\sum_{p=0}^{+\infty}\frac{(-1)^p}{p!(p+2)!}\Big(\frac{r}{2}\Big)^{2+2p}\big(\kappa_{\mathrm{s}}^{4+2p} - \kappa_{\mathrm{p}}^{4+2p}\big)\big(\phi(p)+\phi(p+2)\big), \tag{4.7}$$

$$\gamma_3(s,t) = \kappa_{\mathrm{s}}^3 rF(\kappa_{\mathrm{s}}, s, t)J_3(\kappa_{\mathrm{s}} r) - \kappa_{\mathrm{p}}^3 rF(\kappa_{\mathrm{p}}, s, t)J_3(\kappa_{\mathrm{p}} r) - \frac{2\mathrm{i}}{\pi}\alpha_2 - \frac{\mathrm{i}r^2}{4\pi}\alpha_3 - \frac{\mathrm{i}r}{\pi}\sum_{p=0}^{+\infty}\frac{(-1)^p}{p!(p+3)!}\Big(\frac{r}{2}\Big)^{3+2p}\big(\kappa_{\mathrm{s}}^{6+2p} - \kappa_{\mathrm{p}}^{6+2p}\big)\big(\phi(p)+\phi(p+3)\big), \tag{4.8}$$

and

$$\begin{aligned}\boldsymbol{Z}_2(s,t) = {}& \frac{1}{\pi}\frac{\lambda+\mu}{\lambda+3\mu}\xi(s,t)\boldsymbol{I} + \frac{\mathrm{i}}{2\mu}\big\{\widetilde{\lambda}\boldsymbol{M}_2(s,t) - \widetilde{\mu}\boldsymbol{M}_3(s,t)\big\} \\ & \times\left\{\kappa_{\mathrm{s}}F(\kappa_{\mathrm{s}}, s, t)\frac{J_1(\kappa_{\mathrm{s}} r)}{r} - \frac{\mathrm{i}\kappa_{\mathrm{s}}^2}{2\pi}\sum_{p=0}^{+\infty}\frac{(-1)^p}{p!(p+1)!}\Big(\frac{\kappa_{\mathrm{s}} r}{2}\Big)^{2p}\big(\phi(p)+\phi(p+1)\big)\right\} \\ & - \frac{\mathrm{i}}{2\omega^2}\big\{(\mu+\widetilde{\mu})\boldsymbol{M}_1(s,t) + 4\widetilde{\lambda}\boldsymbol{M}_2(s,t)\big\} \\ & \times\left\{\kappa_{\mathrm{s}}^2F(\kappa_{\mathrm{s}}, s, t)\frac{J_2(\kappa_{\mathrm{s}} r)}{r^2} - \kappa_{\mathrm{p}}^2F(\kappa_{\mathrm{p}}, s, t)\frac{J_2(\kappa_{\mathrm{p}} r)}{r^2}\right. \\ & \qquad \left. - \frac{\mathrm{i}}{4\pi}\sum_{p=0}^{+\infty}\frac{(-1)^p}{p!(p+2)!}\Big(\frac{r}{2}\Big)^{2p}\big(\kappa_{\mathrm{s}}^{4+2p} - \kappa_{\mathrm{p}}^{4+2p}\big)\big(\phi(p)+\phi(p+2)\big)\right\} \\ & + \frac{\mathrm{i}\widetilde{\lambda}}{2\omega^2}\frac{\boldsymbol{M}_2(s,t)}{r} \times\left\{\kappa_{\mathrm{s}}^3F(\kappa_{\mathrm{s}}, s, t)J_3(\kappa_{\mathrm{s}} r) - \kappa_{\mathrm{p}}^3F(\kappa_{\mathrm{p}}, s, t)J_3(\kappa_{\mathrm{p}} r) - \frac{\mathrm{i}r}{4\pi}\alpha_3\right. \\ & \qquad \left. - \frac{\mathrm{i}}{\pi}\sum_{p=0}^{+\infty}\frac{(-1)^p}{p!(p+3)!}\Big(\frac{r}{2}\Big)^{3+2p}\big(\kappa_{\mathrm{s}}^{6+2p} - \kappa_{\mathrm{p}}^{6+2p}\big)\big(\phi(p)+\phi(p+3)\big)\right\}.\end{aligned} \tag{4.9}$$

By a straightforward calculation and [4, Section 7.1.3], we have

$$\frac{r}{|s-t|} \in BC^n(\mathbb{R}^2), \qquad \sqrt{1+f'(t)^2} \in BC^n(\mathbb{R}),$$
$$\boldsymbol{Z}_1(s,t) \in [BC^n(\mathbb{R}^2)]^{2\times 2}, \quad \xi(s,t) \in BC^n(\mathbb{R}^2).$$

Thus, using (4.4)-(4.8), we conclude that

$$\rho_0(\kappa,s,t)\in BC^n(\mathbb{R}^2),\quad \kappa_{\rm s} r\rho_1(\kappa_{\rm s},s,t)\in BC^n(\mathbb{R}^2),$$
$$\gamma_1(s,t)\in BC^n(\mathbb{R}^2),\qquad \gamma_2(s,t)\in BC^n(\mathbb{R}^2),\quad \gamma_3(s,t)\in BC^n(\mathbb{R}^2).$$

By a careful observation from (4.9), we have $\boldsymbol{Z}_2(s,t)\in[BC^n(\mathbb{R}^2)]^{2\times 2}$. Since

$$\boldsymbol{A}_3(s,t)=\boldsymbol{A}_4(s,t)-\boldsymbol{A}_5(s,t),$$

it follows from the smoothness of $\boldsymbol{\Psi}(\mathbf{x},\mathbf{y}')$ and $\boldsymbol{U}(\mathbf{x},\mathbf{y})$ for $\mathbf{x},\mathbf{y}\in U_h$ that $\boldsymbol{A}_3(s,t)$ is smooth. These, together with (4.3), imply that $C^*(s,t)\in[BC^n(\mathbb{R}^2)]^{2\times 2}$. Thus, the condition **C2** holds.

For the condition **C3**, it follows from [3, Theorem 2.1(c), Theorem 2.3(a)] that the elements of $\boldsymbol{G}$ and $\boldsymbol{\Pi}$ satisfy

$$\max_{j,k=1,2}|G_{jk}(\mathbf{x},\mathbf{y})|\lesssim\frac{1+(\mathrm{x}_2-h)(\mathrm{y}_2-h)}{|\mathrm{x}_1-\mathrm{y}_1|^{3/2}},\tag{4.10}$$

$$\max_{j,k=1,2}|\Pi_{jk}(\mathbf{x},\mathbf{y})|\lesssim\frac{1+(\mathrm{x}_2-h)(\mathrm{y}_2-h)}{|\mathrm{x}_1-\mathrm{y}_1|^{3/2}}\tag{4.11}$$

for any $\mathbf{x},\mathbf{y}\in U_h$ with $|\mathrm{x}_1-\mathrm{y}_1|\geq\varepsilon>0$. Since the columns of $\boldsymbol{G}(\cdot,\mathbf{y})$ and the columns of $\boldsymbol{\Pi}(\cdot,\mathbf{y})$ are solutions to Navier equation in $U_h\backslash\{\mathbf{y}\}$ (see [3, Theorem 2.3(c)]), a direct application of [1, Lemma 2.5] implies that the estimates (4.10) and (4.11) actually hold for partial derivatives of $\boldsymbol{G}(\mathbf{x},\mathbf{y})$ and $\boldsymbol{\Pi}(\mathbf{x},\mathbf{y})$ of any order. Note that $\boldsymbol{A}(s,t)$ is related to $\boldsymbol{G}(\mathbf{x},\mathbf{y})$, $\boldsymbol{\Pi}(\mathbf{x},\mathbf{y})$ and their derivatives, thus the condition **C3** holds with $p=3/2$ and $C>0$ only depends on c_1. The proof is complete. □

Remark 4.1. From the proof of Theorem 4.1, it easily follows that $\boldsymbol{B}(s,t)\in C^n_{0,\pi}(\mathbb{R}^2)$ and $\boldsymbol{C}(s,t)\in BC^n_p(\mathbb{R}^2)$ with $p=3/2$ if $f\in B^{(n+2)}_{c_1,c_2}$.

5. Numerical Results

The purpose of this section is to illustrate the feasibility of the Nyström method by several numerical examples. As presented in (2.6), the expression of $\boldsymbol{G}_H(\mathbf{x},\mathbf{y})$ involves the matrix function $\boldsymbol{U}(\mathbf{x},\mathbf{y})$ which is smooth on the boundary Γ. However, $\boldsymbol{U}(\mathbf{x},\mathbf{y})$ is given in terms of an improper integral on the infinite interval which is difficult to compute numerically. Thus in the numerical experiments, we replace $\boldsymbol{G}_H(\mathbf{x},\mathbf{y})$ arising in (2.11) by $\boldsymbol{\Psi}(\mathbf{x},\mathbf{y})-\boldsymbol{\Psi}(\mathbf{x},\mathbf{y}')$ to avoid the complicated computation of $\boldsymbol{U}(\mathbf{x},\mathbf{y})$. It is shown that the numerical experiments are indeed satisfactory by using this replacement.

In the following examples, we assume that the Lamé constants $\lambda=1,\mu=1$. For the Nyström method of the integral equation (4.1), we truncate the infinite interval $(-\infty,+\infty)$ into a finite interval $(-R,R)$. Setting $s=t_j$ for $j=0,1,2,\ldots,2NR/\pi$ in (4.2) gives a linear system of equations which can be solved to obtain the density $\widetilde{\boldsymbol{\psi}}_N$, and then we can calculate the solution $\boldsymbol{u}^{\rm sc}$ through (2.9). In each example, we compute the scattered field at random points $z_i, i=1,\ldots,Nb$ in the region $[-2.5,2.5]\times[0.5,1.5]$, where the number of random points $Nb=101$. See the blue points in Fig. 5.1 for the geometry profile. To investigate the performance of our algorithm, we will compute the following relative error:

$$E(\boldsymbol{u}^{\rm sc}):=\frac{\left[\sum_{i=1}^{Nb}|\boldsymbol{u}^{\rm sc}(z_i)-\boldsymbol{u}^{\rm sc,app}(z_i)|^2\right]^{1/2}}{\left[\sum_{i=1}^{Nb}|\boldsymbol{u}^{\rm sc}(z_i)|^2\right]^{1/2}},$$

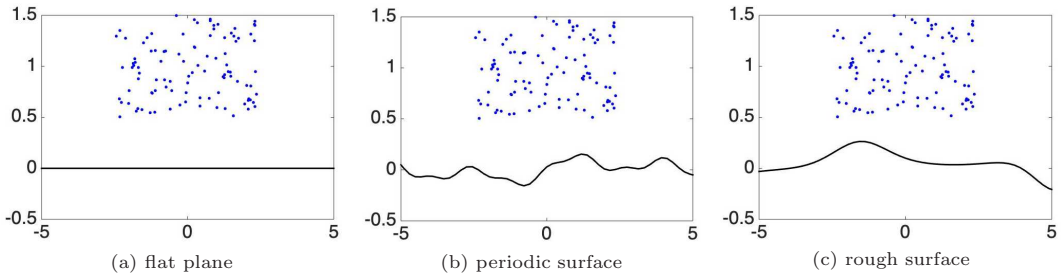

(a) flat plane (b) periodic surface (c) rough surface

Fig. 5.1. The solid lines in (a)-(c) represent the profile of the scattering interface for Examples 5.1-5.3, respectively, and the scattered field is computed on the blue random points in the region $[-2.5, 2.5] \times [0.5, 1.5]$.

where $\boldsymbol{u}^{\mathrm{sc,app}}(z_i)$ denotes the approximate value of $\boldsymbol{u}^{\mathrm{sc}}(z_i)$ which is computed by our Nyström method.

Example 5.1. We consider the elastic scattering by a planar $f(\mathrm{x}_1) = 0$ with an incident plane wave. The profile of the flat surface is given in Fig. 5.1(a). In general, an elastic plane wave can be written as a linear combination of a compressional plane wave $\boldsymbol{u}_{\mathrm{p}}^{\mathrm{inc}}(\mathbf{x};\boldsymbol{\theta})$ and a shear plane wave $\boldsymbol{u}_{\mathrm{s}}^{\mathrm{inc}}(\mathbf{x};\boldsymbol{\theta})$, that is

$$\boldsymbol{u}^{\mathrm{inc}}(\mathbf{x};\boldsymbol{\theta}) = \alpha \boldsymbol{u}_{\mathrm{p}}^{\mathrm{inc}}(\mathbf{x};\boldsymbol{\theta}) + \beta \boldsymbol{u}_{\mathrm{s}}^{\mathrm{inc}}(\mathbf{x};\boldsymbol{\theta}), \quad \alpha, \beta \in \mathbb{C}, \tag{5.1}$$

where $\boldsymbol{u}_{\mathrm{p}}^{\mathrm{inc}}(\mathbf{x};\boldsymbol{\theta}) = \boldsymbol{\theta} e^{\mathrm{i}\kappa_{\mathrm{p}}\mathbf{x}\cdot\boldsymbol{\theta}}$ and $\boldsymbol{u}_{\mathrm{s}}^{\mathrm{inc}}(\mathbf{x};\boldsymbol{\theta}) = \boldsymbol{\theta}^{\perp} e^{\mathrm{i}\kappa_{\mathrm{s}}\mathbf{x}\cdot\boldsymbol{\theta}}$ with $\boldsymbol{\theta} \in \mathbb{S} := \{\mathbf{x} \in \mathbb{R}^2 : |\mathbf{x}| = 1\}$ being an incident direction. In this example, we choose $\boldsymbol{\theta} = (0, -1)^{\top}$. We consider the case $(\alpha, \beta) = (1, 1)$ in (5.1), then the corresponding incident wave is

$$\boldsymbol{u}_1^{\mathrm{inc}}(\mathbf{x}) = (-e^{-\mathrm{i}\kappa_{\mathrm{s}}\mathrm{x}_2}, -e^{-\mathrm{i}\kappa_{\mathrm{p}}\mathrm{x}_2})^{\top}.$$

Since the rough surface is given by a planar $f(\mathrm{x}_1) = 0$, it is easily seen that the corresponding scattered fields can be written explicitly as

$$\boldsymbol{u}_1^{\mathrm{sc}}(\mathbf{x}) = (e^{\mathrm{i}\kappa_{\mathrm{s}}\mathrm{x}_2}, e^{\mathrm{i}\kappa_{\mathrm{p}}\mathrm{x}_2})^{\top}. \tag{5.2}$$

Table 5.1 presents the relative error $E(\boldsymbol{u}_1^{\mathrm{sc}})$ for the case $R = 10\pi, \omega = 10, h = -10$ and the case $R = 20\pi, \omega = 10, h = -10$, where R is the truncation index, ω is the frequency, and h is the index in (2.9). It can be seen from Table 5.1 that the relative error converges as N increases and as expected, a larger R will lead to faster convergence.

Table 5.1: Relative error against N for Example 5.1 with a planar surface.

N	$R = 10\pi, \omega = 10, h = -10$	$R = 20\pi, \omega = 10, h = -10$
	$E(\boldsymbol{u}_1^{\mathrm{sc}})$	$E(\boldsymbol{u}_1^{\mathrm{sc}})$
16	0.0227189017	0.0143637141
32	0.0131962110	0.0081907240
64	0.0075534247	0.0045372560
128	0.0044238280	0.0024815277

Example 5.2. We consider the elastic scattering by a periodic unbounded rough surface with the periodic surface given by

$$f(\mathrm{x}_1) = 0.084\sin(0.6\pi\mathrm{x}_1) + 0.084\sin(0.24\pi\mathrm{x}_1) + 0.03\sin\big(1.5\pi(\mathrm{x}_1 - 1)\big).$$

See the profile of this periodic surface in Fig. 5.1(b). The incident wave is chosen to be

$$\boldsymbol{u}_2^{\mathrm{inc}}(\mathbf{x}) = \boldsymbol{\Psi}(\mathbf{x}, \mathbf{z})\boldsymbol{d} \tag{5.3}$$

with the point $\mathbf{z} = (0, -3)$ and the polarization direction $\boldsymbol{d} = (0.6, 0.8)^\top$. Due to the fact that the point $\mathbf{z}$ is below the surface Γ, it follows from the well-posedness of the problem (DP) that the corresponding scattered field has the explicit expression

$$\boldsymbol{u}_2^{\mathrm{sc}}(\mathbf{x}) = -\boldsymbol{\Psi}(\mathbf{x}, \mathbf{z})\boldsymbol{d}, \quad \mathbf{x} \in \Omega. \tag{5.4}$$

Table 5.2 presents the relative error $E(\boldsymbol{u}_2^{\mathrm{sc}})$ against N for the case $R = 20\pi, \omega = 5, h = -10$ and the case $R = 20\pi, \omega = 10, h = -10$. It can be observed from Table 5.2 that the Nyström method can provide satisfactory numerical results for the considered two cases, and compared with the low frequency $\omega = 5$, the convergence is slower at the high frequency $\omega = 10$.

Table 5.2: Relative error against N for Example 5.2 with a periodic surface.

N	$R = 20\pi, \omega = 5, h = -10$	$R = 20\pi, \omega = 10, h = -10$
	$E(\boldsymbol{u}_2^{\mathrm{sc}})$	$E(\boldsymbol{u}_2^{\mathrm{sc}})$
16	0.0011482973	0.0033226157
32	0.0006254735	0.0017469835
64	0.0003292870	0.0009710596
128	0.0001721390	0.0005278299

Example 5.3. We consider the elastic scattering by a non-periodic unbounded rough surface given by

$$f(\mathrm{x}_1) = 0.1\cos\big(0.1\mathrm{x}_1^2\big)e^{-\sin(\mathrm{x}_1)}.$$

See the profile of this rough surface in Fig. 5.1(c). We choose the same incident wave $\boldsymbol{u}_3^{\mathrm{inc}}(\mathbf{x})$ as in (5.3). Similar as in Example 5.2, the corresponding scattered field $\boldsymbol{u}_3^{\mathrm{sc}}$ has the form (5.4). Table 5.3 presents the relative error $E(\boldsymbol{u}_3^{\mathrm{sc}})$ against N for the case $R = 20\pi, \omega = 5, h = -10$ and the case $R = 20\pi, \omega = 5, h = -50$. As shown in Table 5.3, the relative error converges as N increases and the case $h = -10$ can provide faster convergence than the case $h = -50$.

Table 5.3: Relative error against N for Example 5.3 with a non-periodic surface.

N	$R = 20\pi, \omega = 5, h = -10$	$R = 20\pi, \omega = 5, h = -50$
	$E(\boldsymbol{u}_3^{\mathrm{sc}})$	$E(\boldsymbol{u}_3^{\mathrm{sc}})$
16	0.0012602860	0.0021020358
32	0.0006790257	0.0011670703
64	0.0003618276	0.0006383604
128	0.0001863967	0.0003486776

6. Conclusion

In this paper, we present a Nyström method for the two-dimensional time-harmonic elastic scattering by unbounded rough surfaces with Dirichlet boundary condition. With the aid of the ascending series expansions of the Bessel functions, we analyze the singularities of the relevant integral kernels. Based on this, we obtain the superalgebraic convergence rate of the Nyström method depending on the smoothness of the rough surfaces. Several numerical examples demonstrate that the numerical solution converges when the number of quadrature points N on the rough surface increases, and the convergence speed is related to the step length π/N, the truncation index R, the frequency ω, and the index h. It should be pointed out that the numerical results presented in Tables 5.1-5.3 do not fully support the superalgebraic convergence established in Theorem 4.1. We think a possible reason is the existence of truncation error and machine accuracy. A possible continuation is to extend the present work to the case of impedance boundary condition or the case of penetrable interface, which will be our future work.

Acknowledgments. This work was partially supported by the National Key R&D Program of China (Grant 2018YFA0702502), by the Beijing Natural Science Foundation (Grant Z210001), by the NNSF of China (Grants 12171057, 12271515, 12201023), by the Youth Innovation Promotion Association CAS, by the Education Department of Hunan Province (Grant 21B0299), by the Fundamental Research Funds for the Central Universities (Grant YWF-23-Q-1026, YWF-22-T-204).

References

[1] T. Arens, *The Scattering of Elastic Waves by Rough Surfaces*, PhD Thesis, Brunel University, 2000.

[2] T. Arens, Uniqueness for elastic wave scattering by rough surfaces, *SIAM J. Math. Anal.*, **33** (2001), 461–476.

[3] T. Arens, Existence of solution in elastic wave scattering by unbounded rough surface, *Math. Meth. Appl. Sci.*, **25** (2002), 507–528.

[4] K. Atkinson, *The Numerical Solution of Integral Equations of the Second Kind*, Cambridge University Press, 1997.

[5] G. Bao and J. Lin, Imaging of local surface displacement on an infinite ground plane: The multiple frequency case, *SIAM J. Appl. Math.*, **71** (2011), 1733–1752.

[6] G. Bao, L. Xu, and T. Yin, An accurate boundary element method for the exterior elastic scattering problem in two dimensions, *J. Comput. Phys.*, **384** (2017), 343–363.

[7] S. Chaillat, M. Bonnet, and J.F. Semblat, A multi-level fast multipole BEM for 3-D elastodynamics in the frequency domain, *Comput. Methods Appl. Mech. Engrg.*, **197** (2008), 4233–4249.

[8] S.N. Chandler-Wilde and J. Elschner, Variational approach in weighted Sobolev spaces to scattering by unbounded rough surfaces, *SIAM J. Math. Anal.*, **42** (2010), 2554–2580.

[9] S.N. Chandler-Wilde and P. Monk, Existence, uniqueness, and variational methods for scattering by unbounded rough surfaces, *SIAM J. Math. Anal.*, **37** (2005), 598–618.

[10] S.N. Chandler-Wilde and P. Monk, The PML for rough surface scattering, *Appl. Numer. Math.*, **59** (2009), 2131–2154.

[11] S.N. Chandler-Wilde and C.R. Ross, Scattering by rough surfaces: The Dirichlet problem for the Helmholtz equation in a non-locally perturbed half-plane, *Math. Methods Appl. Sci.*, **19** (1996), 959–976.

[12] S.N. Chandler-Wilde, C.R. Ross, and B. Zhang, Scattering by infinite one-dimensional rough surfaces, *Proc. Math. Phys. Eng. Sci.*, **455** (1999), 3767–3787.
[13] S.N. Chandler-Wilde, B. Zhang, and C.R. Ross, On the solvability of second kind integral equations on the real line, *J. Math. Anal. Appl.*, **245** (2000), 28–51.
[14] D. Colton and R. Kress, *Inverse Acoustic and Electromagnetic Scattering Theory*, Springer, 2019.
[15] M. Ding, J. Li, K. Liu, and J. Yang, Imaging of locally rough surfaces by the linear sampling method with the near-field data, *SIAM J. Imaging Sci.*, **10** (2017), 1579–1602.
[16] H. Dong, J. Lai, and P. Li, A highly accurate boundary integral method for the elastic obstacle scattering problem, *Math. Comp.*, **90** (2021), 2785–2814.
[17] H. Dong, J. Lai, and P. Li, A spectral boundary integral method for the elastic obstacle scattering problem in three dimensions, *J. Comput. Phys.*, **469** (2022), 111546.
[18] J. Elschner and G. Hu, Elastic scattering by unbounded rough surfaces, *SIAM J. Math. Anal.*, **44** (2012), 4101–4127.
[19] R. Kress, On the numerical solution of a hypersingular integral equation in scattering theory, *J. Comput. Appl. Math.*, **61** (1995), 345–360.
[20] J. Li and G. Sun, A nonlinear integral equation method for the inverse scattering problem by sound-soft rough surfaces, *Inverse Probl. Sci. Eng.*, **23** (2015), 557–577.
[21] J. Li, G. Sun, and R. Zhang, The numerical solution of scattering by infinite rough interfaces based on the integral equation method, *Comput. Math. Appl.*, **71** (2016), 1491–1502.
[22] J. Li, J. Yang, and B. Zhang, A linear sampling method for inverse acoustic scattering by a locally rough interface, *Inverse Probl. Imaging*, **15** (2021), 1247–1267.
[23] F.L. Louër, A high order spectral algorithm for elastic obstacle scattering in three dimensions, *J. Comput. Phys.*, **279** (2014), 1–18.
[24] W. McLean, *Strongly Elliptic Systems and Boundary Integral Equations*, Cambridge University Press, 2000.
[25] A. Meier, T. Arens, S.N. Chandler-Wilde, and A. Kirsch, A Nyström method for a class of integral equations on the real line with applications to scattering by diffraction gratings and rough surfaces, *J. Integral Equations Appl.*, **12** (2000), 281–321.
[26] D. Natroshvili, T. Arens, and S.N. Chandler-Wilde, Uniqueness, existence, and integral equation formulations for interface scattering problems, *Mem. Differ. Equ. Math. Phys.*, **30** (2003), 105–146.
[27] C.R. Ross, *Direct and Inverse Scattering by Rough Surfaces*, PhD Thesis, Brunel University, 1996.
[28] M.S. Tong and W.C. Chew, Nyström method for elastic wave scattering by three-dimensional obstacles, *J. Comput. Phys.*, **226** (2007), 1845–1858.
[29] B. Zhang and S.N. Chandler-Wilde, Integral equation methods for scattering by infinite rough surfaces, *Math. Methods Appl. Sci.*, **26** (2003), 463–488.